UCRL-????

How Accurately Can We Calculate Neutrons Slowing Down In Water?

by
Dermott E. Cullen, LLNL
Roger N. Blomquist, ANL
Maurice Greene, ORNL
Edward Lent, LLNL
Robert MacFarlane, LANL
Scott McKinley, LLNL
Ernest F. Plechaty, LLNL
Jean Christophe Sublet, CEA

Contact
Dermott E. Cullen
University of California
Lawrence Livermore National Laboratory
P.O.Box 808/L-159
Livermore, CA 94550

Tele: 925-423-7359
E.Mail: cullen1@llnl.gov
Website: http://www.llnl.gov/cullen1

April 1, 2006

U.S. Department of Energy
Lawrence Livermore National Laboratory

DISCLAIMER

Work performed under the auspices of the U. S. Department of Energy by the University of California Lawrence Livermore National Laboratory under Contract W-7405-Eng-48.

UCRL-????

How Accurately Can We Calculate Neutrons Slowing Down In Water?

by
Dermott E. Cullen, LLNL
Roger N. Blomquist, ANL
Maurice Greene, ORNL
Edward Lent, LLNL
Robert MacFarlane, LANL
Scott McKinley, LLNL
Ernest F. Plechaty, LLNL
Jean Christophe Sublet, CEA

Contact
Dermott E. Cullen
University of California
Lawrence Livermore National Laboratory
P.O.Box 808/L-159
Livermore, CA 94550

Tele: 925-423-7359
E.Mail: cullen1@llnl.gov
Website: http://www.llnl.gov/cullen1

April 1, 2006

Introduction

We have compared the results produced by a variety of currently available Monte Carlo neutron transport codes for the relatively simple problem of a fast source of neutrons slowing down and thermalizing in water. Initial comparisons showed rather large differences in the calculated flux; up to 80% differences. By working together we iterated to improve the results by: 1) insuring that all codes were using the same data, 2) improving the models used by the codes, and 2) correcting errors in the codes; no code is perfect.

Even after a number of iterations we still found differences, demonstrating that our Monte Carlo and supporting codes are far from perfect; in particularly we found that the often overlooked nuclear data processing codes can be the weakest link in our systems of codes.

The results presented here represent the **today's state-of-the-art**, in the sense that all of the Monte Carlo codes are modern, widely available and used codes. They all use the most up-to-date nuclear data, and the results are very recent, weeks or at most a few months old; these are the results that current users of these codes should expect to obtain from them. As such, the accuracy and limitations of the codes presented here should serve as guidelines to code users in interpreting their results for similar problems.

We avoid crystal ball gazing, in the sense that we limit the scope of this report to what is available to code users **today**, and we avoid predicting future improvements that may or may not actual come to pass. An exception that we make is in presenting results for an improved thermal scattering model currently being testing using advanced versions of NJOY and MCNP that are not currently available to users, but are planned for release in the not too distant future. The other exception is to show comparisons between experimentally measured water cross sections and preliminary ENDF/B-VII thermal scattering law, $S(\alpha,\beta)$ data; although these data are strictly preliminary they are currently available and undergoing testing and these results were judged to be within the scope of this report.

Overview

In an earlier paper titled "How Accurately can we Calculate Thermal Systems" [1] we compared K-eff calculated by a number of neutron transport codes, mostly Monte Carlo codes, for a series of theoretical pin-cell assemblies, and we found a rather large spread in the answers, as shown in the table below from reference [1]. Three (3) pin-cells were calculated with 1/2", 1/4", and 1/8" radius uranium pins, using free atom or bound atom thermal scattering law data [2], for a total of six (6) cases, as shown in the table below; for details, see [1].

Why theoretical rather than experimentally measured systems? Sorry to say that human nature is such that if we know the answer to a given problem today's codes allow us enough flexibility to dial in almost any answer we want. By using only theoretical systems where none of the participants knew the answer in advance, we can attempt to avoid this unfortunate potential bias.

K-eff for Monte Carlo Codes from Reference [1]

Case #	Code	1/2" Free	1/2" Bound	1/4" Free	1/4" Bound	1/8" Free	1/8" Bound
1	COG(Mark)	1.0112(12)	0.9636(12)	1.0111(12)	0.9159(12)	1.0109(12)	0.9019(12)
2	COG(Dave)	1.0115(12)	0.9608(12)	1.0121(12)	0.9148(12)	1.0133(12)	0.9065(12)
3	KENO(Dave)	1.0092(38)	0.9628(5)	1.0133(7)	0.9163(7)	1.0133(8)	0.9050(7)
4	MCNP5(Bob)	1.01283(12)	0.96062(13)	1.01078(16)	0.91221(18)	1.01206(22)	0.89867(23)
5	MCNP5(Mark)	1.01236(38)	0.96073(42)	1.01015(52)	0.91115(55)	1.01200(68)	0.89911(70)
6	MCNP5(Red)	1.01294(40)	0.96059(42)	1.01133(56)	0.91204(58)	1.01299(74)	0.89932(73)
7	MCNP5(Red)	1.01298(13)	0.96046(14)	1.01089(17)	0.91208(18)	1.01187(23)	0.89854(23)
8	MCNP5(Red)	1.01279(4)	0.96067(4)	1.01094(6)	0.91212(6)	1.01187(7)	0.89882(8)
9	MCNP4C(Dave)	1.0101(05)	0.9597(06)	1.0105(08)	0.9133(08)	1.0103(09)	0.9027(11)
10	MCNP4B(Andrej)	1.01071(6)	0.96061(6)	1.00932(9)	0.91380(9)	1.01038(11)	0.90201(11)
11	MCNPX21(Andrej)	1.01075(6)	0.96071(7)	1.00927(8)	0.91402(9)	1.01023(11)	0.90199(11)
12	MCNPX24(Andrej)	--	0.96071(6)	--	--	--	--
13	MCNPX24(Andrej)	1.01292(6)	0.96211(7)	1.01100(9)	0.91496(9)	1.01178(11)	0.90264(11)
14	MCNPX24(Andrej)	1.01292(6)	0.96055(6)	1.01100(9)	0.91207(9)	1.01178(11)	0.89874(12)
15	MCNPX24(Andrej)	1.01292(6)	0.96044(6)	1.01100(9)	0.91167(9)	1.01178(11)	0.89850(11)
16	MCU(Mikhail)	--	0.96284(35)	--	0.91454(50)	--	0.89653(56)
17	MCU(Mikhail)	1.01680(30)	0.96378(30)	1.01632(40)	0.91404(40)	1.01556(40)	0.89842(30)
18	MONK8B(Chris)	1.01300(5)	0.95990(5)	1.01130(5)	0.91140(5)	1.0132(2)	0.8991(1)
19	MONK9(Chris)	1.0136(3)	0.9593(3)	1.0117(2)	0.9101(2)	1.0121(2)	0.8969(1)
20	MVP(Yasunobu)	1.01299(8)	0.96065(9)	1.01169(12)	0.91309(15)	1.01282(17)	0.90016(19)
23	TART04(Red)	1.00916(50)	0.96114(50)	1.00983(50)	0.91548(50)	1.01072(50)	0.90333(50)
24	TART04(Red)	1.00952(5)	0.96071(5)	1.00933(5)	0.91544(5)	1.01091(5)	0.90293(5)
25	TART04(Mark)	1.0101(4)	0.9598(5)	1.0098(7)	0.9138(8)	1.0126(10)	0.9007(11)
26	TART04(Mark)	1.00960(4)	0.96073(4)	1.00926(7)	0.91537(8)	1.01097(10)	0.90312(11)
27	TRIPOLI4(Yi)	1.01295(11)	0.96046(10)	1.01243(10)	0.91197(10)	1.01448(11)	0.89766(10)
28	VIM(Dave)	1.0157(8)	0.9609(8)	1.0150(09)	0.9131(09)	1.0168(11)	0.9020(11)
29	VIM(Roger)	1.00525(7)	0.95939(7)	1.00680(9)	0.90877(9)	1.03463(10)	0.89629(10)
	Average	**1.011792**	**0.960915**	**1.011046**	**0.913212**	**1.013173**	**0.900503**
	Minimum	**1.005250**	**0.959300**	**1.006800**	**0.908770**	**1.010230**	**0.896290**
	Maximum	**1.016800**	**0.963780**	**1.016320**	**0.916300**	**1.034630**	**0.906500**
	Spread	**0.011550**	**0.004480**	**0.009520**	**0.007530**	**0.024400**	**0.010210**

These results was surprising to some people who before this study assumed that today our nuclear data files and our Monte Carlo codes are so accurate that they would all produce "the exact answer". As the above results prove, this is not true; rather than the 0.1% differences that were expected, the table above shows over 1% in the spread in the answers, for a simple integral quantity, K-eff. These are all well

known and respected codes, so we feel this truly represents the state of answers that we can expect.

This study was aimed solely at assessing the current state of our codes and data; trying to determine the sources of these differences was judged to be beyond the scope of this study. However, naturally as soon as these results were published people began asking: how can these results be so different, particularly when a number of these codes claim to be using exactly the same nuclear data? In this case shouldn't all Monte Carlo codes produce the same, right answers? Unfortunately the answer to this question is: no they cannot, because of a number of factors. When we include nuclear data, here is a brief summary of the sources of differences.

1) **Nuclear Data** – Naturally the results from any code cannot be any better than the data that it uses. Today our nuclear data are much better than it was decades ago, and different data bases (e.g., ENDF/B, JEF, JENDL,…) tend to have evaluated data that are very similar, but there are still important differences between these data bases, and they are still evolving and changing. For example, currently a new ENDF/B-VII data base is being developed to replace the currently generally available ENDF/B-VI library. You should ask yourself: if ENDF/B-VI is so good, why is it being replaced?

2) **Nuclear data processing codes** – This seems to be the invisible, or forgotten, step between our nuclear data bases and our transport codes, and yet we have found that this can be the most critical part and weakest link of our code systems, as far as limiting the accuracy of the data used by our Monte Carlo codes, and thereby limiting the accuracy of the results produced by our Monte Carlo codes.

3) **Monte Carlo codes** – Aren't our Monte Carlo codes more or less perfect? Far from it. Compared to deterministic codes, Monte Carlo codes have the advantage of being able to more accurately model geometry, but they are still limited by the accuracy of the nuclear data they use, how data are presented to them by nuclear data processing codes, and ultimately how they interpret data. This limitation can severely affect the results produced by our Monte Carlo codes.

4) **User Selected Input Options** – Our codes (data processing and Monte Carlo) have far too many options, or "dials", that users can, and do, use to affect answers. You can see this from the table above, where we have multiple results for the same Monte Carlo code, submitted by different users. You might assume that if several different people use the same code and nuclear data to calculate the same problem they have to get the same answer. Yet the results in the table above prove that this is not the case.

Slowing Down in Water

Once our study of these thermal pin-cells was completed we turned our focus to determining the source of differences in the calculated results from these code, in the hope of being able to eventually eliminate these differences.

Physically and mathematically the pin cells that we investigated are quite complicated, involving a combination of cylindrical and planar geometry to represent an infinite array of pin cells (this eliminated any effects of overall leakage from the systems), and involved uranium of various enrichments inside the pins, and water outside the pins, filling the remainder of the cell; see [1] for details. An extremely important component of these pin cells was modeling the slowing down in water of the fast neutrons produced by fission in the uranium.

As a first step to determining the sources of differences between our codes we decided to model a much simpler system, namely: the slowing down of a source of fast neutrons in a sphere of water. Here there is no fission, so there is no feedback from slow neutrons back to high energy; the neutron just slow down until they thermalize. We initially thought this must be a trivial problem to solve; unfortunately we were wrong, which is what led to producing this report.

The specifications for the problem are,

1) A 30 cm radius sphere.
2) Filled with water at a density of 1 gram/cc, at room temperature, where water is 2 atoms of H1 to 1 atom of O16; only these 2 materials are involved.
3) Use ONLY the ENDF/B-VI, Release 8 data.
4) There is a time independent (continuous in time), isotropic, point source of neutrons located at the origin of the sphere. It is monoenergetic with an energy of 14.1 MeV.
5) Calculate two separate cases, one using free atom scattering data and the other using bound, thermal scattering law data.
6) Tally both scalar flux within the source, and leakage (scalar current) leaking from the surface of the sphere.
7) Use the TART 616 tally bins, which are equally spaced in lethargy, with 50 bins per energy decade, between 10^{-5} eV up to 20 MeV.
8) Send results to me (D.E. Cullen), in any simple tabulated, text format, and I will compare your results to everybody else's results.

We thought this would be a trivial exercise merely to verify that slowing down in water could not possibly be a source of differences. Boy, were we in for a shock. The first few comparisons we ran showed enormous differences in the results. In our series of code comparisons whenever possible we try at avoid embarrassing any participants, so we will not identify any specific code(s) as having a specific

problem; we will merely briefly state that most of the codes had coding errors that affected results, and some were using very different nuclear data. Both coding error and nuclear data produced enormous initial differences in the results from the participating codes. Most of these sources of differences were eliminated before the final round of comparisons; only the final results are presented here.

I (D.E. Cullen) invited as many codes as possible to participate in this comparison exercise, and we now have Monte Carlo results for the following codes, with results submitted by the indicated contributors, in alphabetical code order,

	Code (Institute)	**Contributor**
1)	COG (LLNL) [3]	Edward Lent
2)	MCNP5 (LANL) [4]	Dermott E. Cullen
3)	MCNPX (LANL) [4]	Dermott E. Cullen
4)	MCNP-Bob (LANL) [5]	Robert MacFarlane
5)	MERCURY (LLNL) [6]	Scott McKinley
6)	TART05 (LLNL) [7]	Ernest F. Plechaty
7)	TRIPOLI (CEA) [8]	Jean Christophe Sublet

Since the results of any code cannot be any better than the data it is using, it is important in a study such as this to examine not only Monte Carlo transport results, but also the cross sections that the codes use. By having both it is often possible to distinguish between differences in Monte Carlo results due to data versus actual errors in the Monte Carlo codes. To aid in this study, we also have cross sections for H bound in H2O for all of the above codes and from,

	Code (Institute)	**Contributor**
8)	AMPX (ORNL) [10]	Maurice Greene
9)	VIM (ANL) [11]	Roger Blomquist

Explanation of Figures

In this report we present many figures; most are in the same format. The upper two-thirds of a figure presents the actual data, and the lower third present the ratio of all data shown in the upper portion of the plot to the first set of data on the plot. Please remember that does not mean that we consider the first set of data to be a standard; our choice is arbitrary and merely convenient so that we can qualitatively see the difference between the sets of data on each plot. In most cases we consider one set of results to be no better or worse than any other set of results, and ultimately we draw no conclusion in this report as to which is best or worse.

What does Slowing Down in Water have to do with Reactor Pin Cells?

The flux spectra in many very different systems are actually quite similar. The figure below compares the flux in a pin cell to the flux in the water flux. Starting at high energy we see differences because in the case of the pin cell the neutron source is due to uranium fission, which produces fast MeV neutrons distributed over a range of energies. In contrast in the water sphere the source is monoenergetic 14.1 MeV neutrons.

Even though these systems have very different neutrons sources, as these neutrons slow down in each system, by about 1 MeV the energy dependent shape of the distributions become very similar and at lower energies both have the same 1/E slowing down spectrum all the way down to below an eV. Below an eV we start to see the effects of thermal scatter, and both go over into a Maxwellian-like thermal spectrum. In the thermal range the main difference between the spectra is that the pin cell is much more absorbing, causing a reduction and shift in its thermal spectrum.

The point of this figure is to illustrate that the spectra in both systems are predominantly defined by neutrons slowing down in water. Therefore our current study focuses on only this aspect of the problem, and removes the complexity of having to deal with fission, and complicated geometry. **Our point is: If your code cannot correctly calculate neutrons slowing down in water, you are likely to have a problem with any system containing water, such as water cooled thermal reactors (PWR or BWR).**

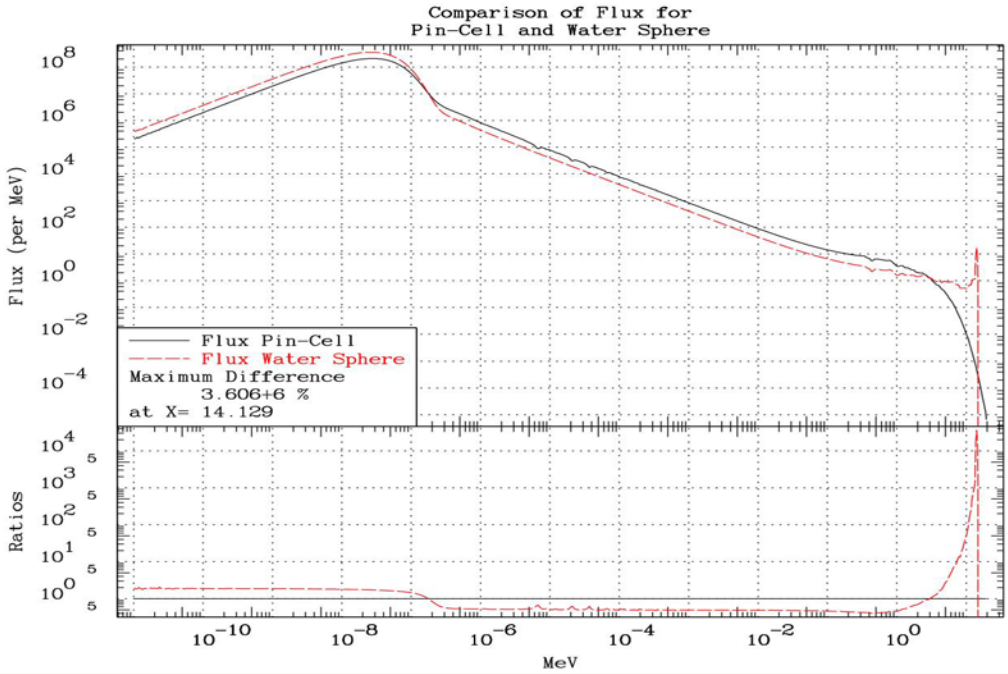

Is Thermal Scattering Important?

For the benefit of those readers who are not familiar with the effect of thermal scattering, here we present results to illustrate its importance. Our first plot shows that without any thermal scattering (Stationary), neutrons continue to slow down in energy and never form a thermal spectrum. In contrast using free atom scattering (Bound), the spectrum begins to differ from the continuous slowing down (Stationary) at about 100 eV and eventually forms a Maxwellian-like thermal spectrum. Note that the integral of the flux without thermal scattering (Stationary) is only about one half the flux with thermal scattering (Bound).

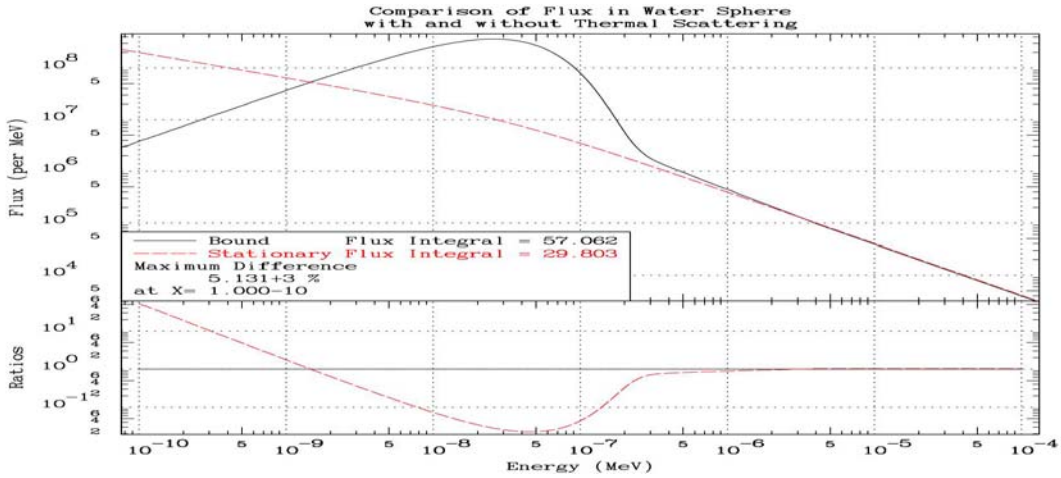

The figure below illustrates the important of using both bound data where we have it (H below 4 eV) and free atom data where we do not (H above 4 eV and O at all energies). Without free atom scattering the spectrum is shifted toward lower energy, due to the continuous slowing down in the H above 4 eV, and O at all energies. Here the effect is obviously not nearly as extreme as when no thermal scattering is used (the figure above), but it is still significant with over 6% difference in the energy dependent flux.

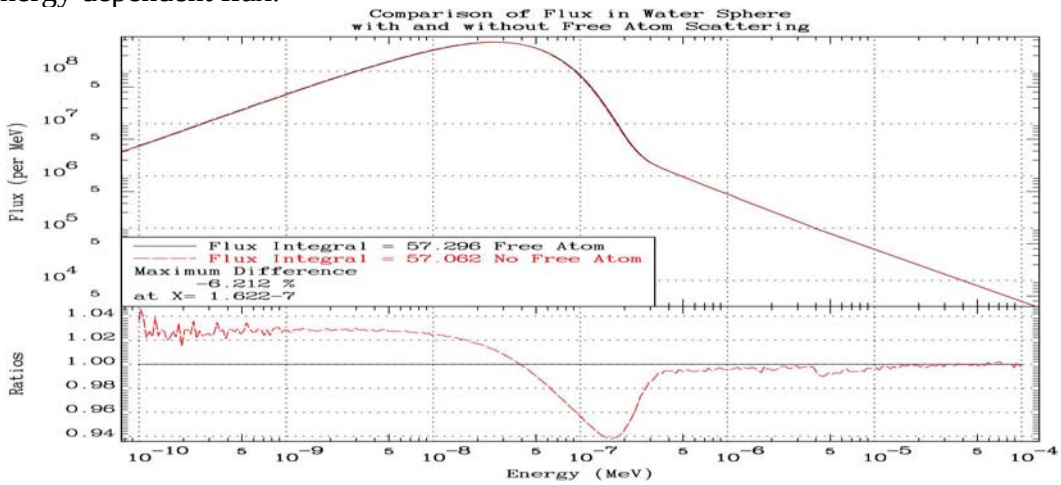

Why study Free and Bound Data Results?

Shouldn't we always use bound data? We recommend that you always use bound data when available, but in most cases data are not available. For example, the ENDF/B-VI, Release 8 data file contains 328 evaluations, for isotopes and elemental mixtures. For these we only have bound thermal scattering law data for a few materials: the list includes: for H bound in H2O, CH2, or ZrH; D in D2O; Be in Be metal or BeO; C in graphite, and O in BeO [2, 10]. That's it; for all other materials to account for thermal scattering we use free atom scattering. For example, in the case of our pin-cell study we used water (H, O), and uranium (U235, U238), and in our current study only water (H, O). In both cases we only have bound data up to 4 eV for H bound in water (H2O), so that in these problems we used free atom scatter for all of the other materials, O, U235, and U238, and H above 4 eV.

Both bound and free data produce similar results, where instead of continuous slowing down (Stationary) due to scatter, they eventually thermalize in a Maxwellian-like distribution, as shown in the figure below. For H bound in H2O the thermal scattering law data only extend up to about 4 eV. Above this energy the bound and free cases use exactly the same data, and therefore produce exactly the same flux, as shown in the figure below.

If you only focus on the upper part of the figure below, it appears that there is very little difference between the bound and free results, but the ratio of free/bound in the lower part of this figure shows that there are important differences in the thermal energy range.

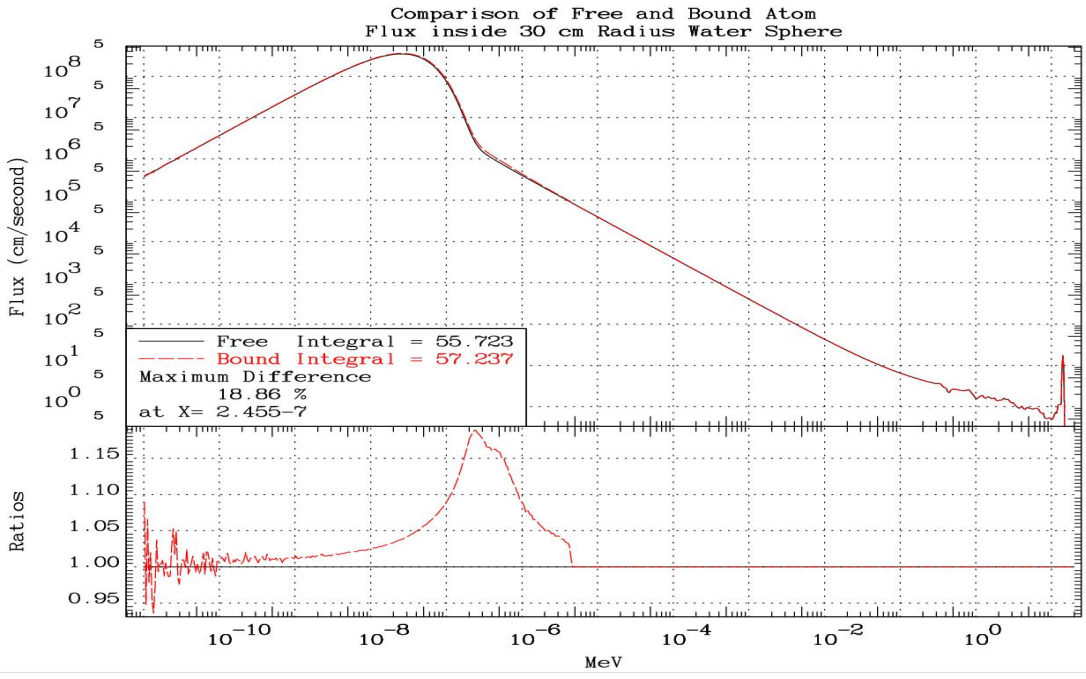

Log scaling is often deceptive in that it can mask important differences. To more clearly see the difference between bound and free results the figure below uses linear scaling, and here we can see the important difference across the peak of the thermal spectrum.

Also note the difference in the integral of the flux: free 55.723, bound 57.237. Remember that above 4 eV the results are identical, so that all of this difference comes from the thermal range. Much of this effect is due to the difference between the free and bound cross sections, with the free cross sections being lower, allowing more leakage and thus less flux within the water. Plots comparing the free and bound cross sections are shown below.

Not so obvious from the figure below, but from the ratio in the lower part of the figure above, we can see that compared to the free data, using bound data shifts the thermal spectrum to slightly higher energy, e.g., the ratio of bound/free is more than unity above the peak of the thermal spectra up to the end of the bound energy range at 4 eV.

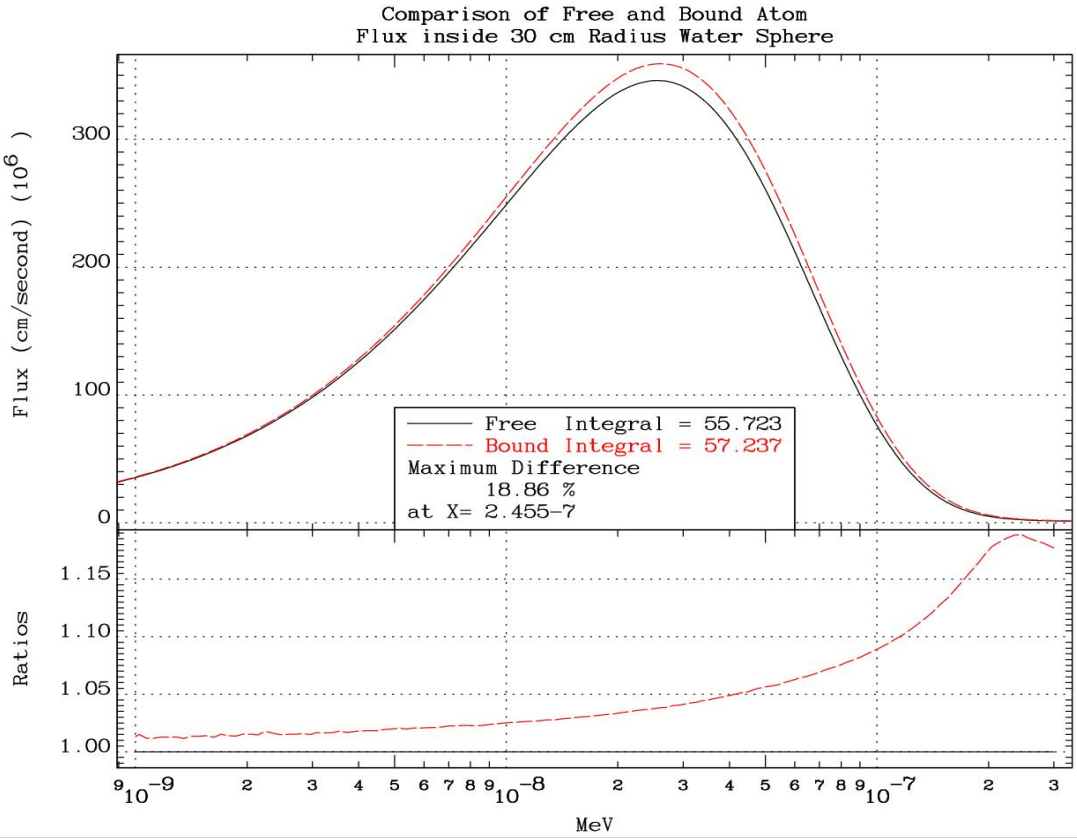

Overview of Water Cross sections

Below we show the water (2 atoms H1 to 1 atom O16) neutron interaction cross sections over the entire energy range from 10^{-11} MeV up to 20 MeV; here we show the free atom cross sections, which are identical to the bound cross sections above about 4 eV. This figure can help us understand the results from our Monte Carlo codes. Remember our problem involves the slowing down of a 14.1 MeV neutron source in a 30 cm radius sphere of water.

From the figure below we can see that: near the source energy 1 mean free path (MFP) is about 10 cm; for a large portion of the energy range from about 10 keV down to 1 eV the cross section is roughly constant and 1 MFP is about 0.67 cm; at lower energies the cross section increases roughly as 1/v (the inverse of the neutron speed) and by 10^{-11} MeV 1 MFP is only about 0.012 cm. Due to this variation in the mean free path we should expect a lot of leakage near the source energy, since the 30 cm radius is here only about 3 MFPs. In the intermediate slowing down range we expect less leakage since the sphere is over 40 MFPs thick, and at very low energy we expect little or no leakage, since by 10^{-11} MeV the sphere is roughly 2500 MFPs thick.

From this figure we can also see that below a few MeV only elastic scatter and capture [n, NO n in this figure] occur, with capture being very small until very low energy. So that over most of the energy range all we have is elastic scatter; what could be simpler to model?

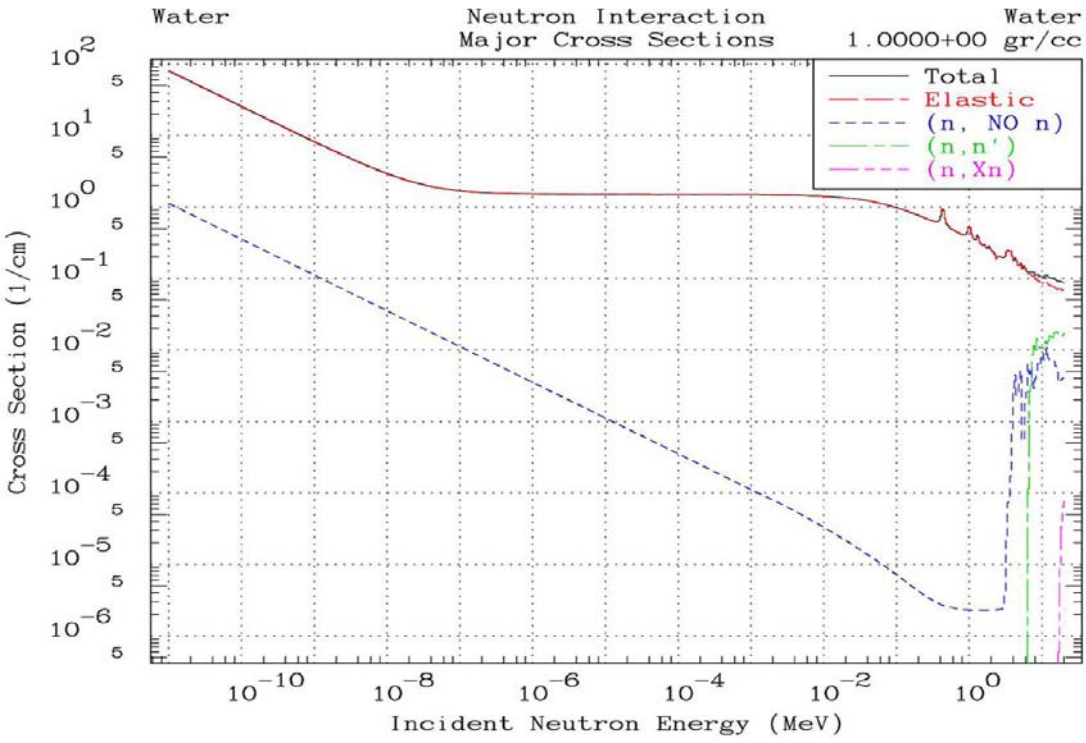

Comparison of H bound in H2O Cross sections

Since the results of any code cannot be any better than the data it is using, it is important in a study such as this to examine not only Monte Carlo transport results, but also the cross sections that the codes use. By having both it is often possible to distinguish between differences in Monte Carlo results due to data versus actual errors in the Monte Carlo codes. We have cross sections for H bound in H2O from seven codes. MCNP5 and MCNPX both use the same NJOY output cross sections, so we need only show the MCNP5 cross sections. MERCURY uses the TART cross sections, so we need only show the TART cross sections.

The first figure below shows the room temperature H bound in H2O cross sections used by the Monte Carlo transport codes compared to free atom cross sections at 293.6 K (room temperature). The bound data only extend up to about 4 eV and above this energy the scatter cross sections are the free atom cross sections; here we are only interested in the energy range up to about 4 eV. The main intent of this figure is to illustrate the rather large difference between the bound and free room temperature cross sections. Note that near the peak of a room temperature thermal spectrum the bound cross sections are 80 % higher than the free cross sections.

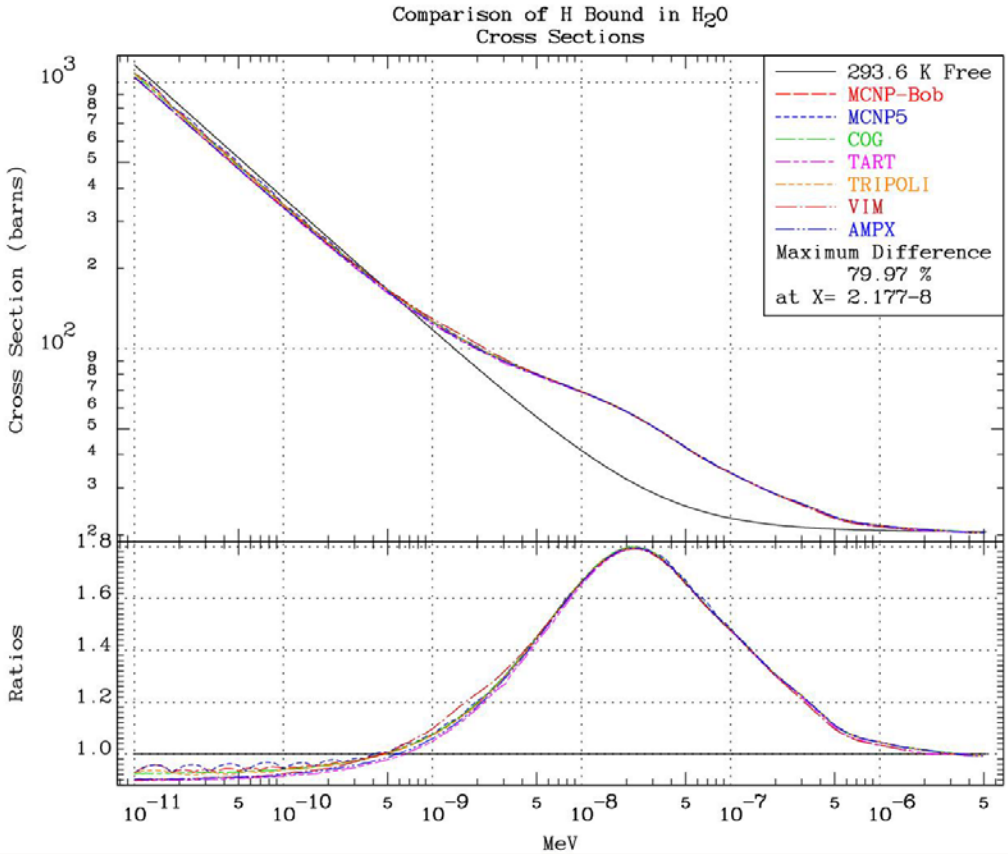

The figure below compares the same data as shown above plus the 0 K free data. In this case the figure only shows the data above 1 eV as we approach the join energy between the bound and free data near 4 eV, where the codes switch from using bound data at lower energy to free data at higher energies. This figure shows the actual data points used (small circles).

Here we see some interesting effects. MCNP-Bob, MCNP5, TRIPOLI and AMPX all approach values that are not only below the 293.6 K free data, but even below the 0 K data. COG approaches the 0 K value. VIM ends at about 1.6 eV. TART approaches the 293.6 K data near 2 eV and then follows it to its joint point near 4 eV. Note also that the codes use different joint energies between the bound and free; VIM near 1.6 eV, TART near 4 eV, COG slightly above 4 eV, MCNP5 and MCNP-Bob near 4.5 eV, TRIPOLI and AMPX near 5 eV.

Based on these differences we should expect differences in the flux near these different join energies. For example, in neutron transport the total reaction rate (the product of the total cross sections times the flux) tends to be smoothly varying, so that any abrupt change in the cross section is compensated by a similar change in the flux in the opposite direction. When we look at the flux calculated by these codes we will see this effect, which can be understood by the discontinuities in the cross sections seen here.

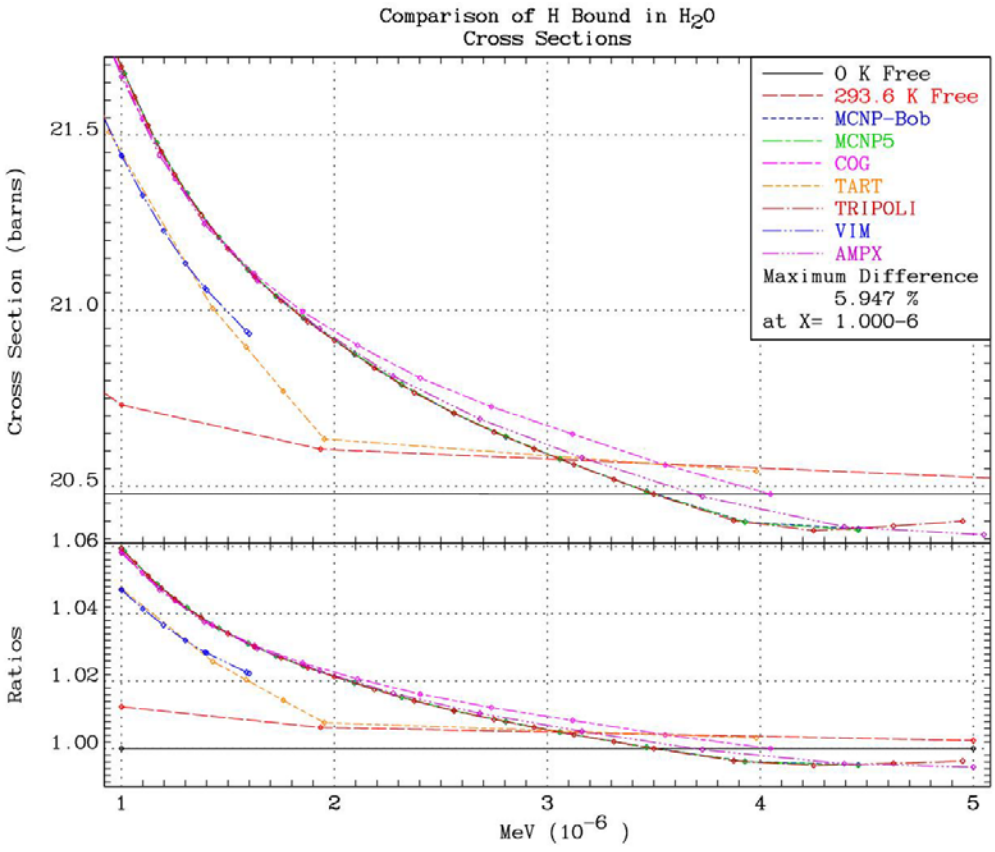

The figure below compares only the seven sets of data used by codes. From this figure we can see a spread in the cross sections of over 6%. The differences are particularly large at low energy, but we also see over 1% differences near the peak of the thermal spectrum, and starting near 0.1 eV up to the joint point near 4 to 5 eV.

We hope this doesn't come as a shock to readers who thought our Monte Carlo codes are perfect. They are far from it, and even the most basic of quantities, such as the scattering cross sections shows fairly large differences. All of these codes claim to be using the same ENDF/B-VI thermal scattering law data, so we cannot blame nuclear data for these differences. **The source of the differences is completely due to the nuclear data processing codes that prepared the cross sections for use by these Monte Carlo codes.**

All of the nuclear data processing codes started from exactly the same ENDF/B-VI thermal scattering law data and they produced scattering cross sections that differ by up to 6% as shown in the figure below. This is just the tip of the iceberg, since you might assume that compared to the difficulty of calculating secondary neutron angular and energy distributions, the cross sections should be trivial to accurately calculate.

For this figure I arbitrarily selected MCNP-Bob as a standard to compare the other cross sections against. This does not mean I assume the MCNP-Bob cross sections are any better or worse than the other sets of cross sections. One of our problems is that we have no idea which, if any, of these sets of cross sections are correct; all we can say is that we see a spread of up to 6% in the cross sections.

It is interesting to note that three of the codes: AMPX, TART and VIM all approach the same low energy limiting values, which is up to 6% lower that the MCNP-Bob cross sections. This effect has been traced to difficulties in obtaining a unique interpretation of the thermal scattering law data based on the ENDF/B formats and procedures manual, ENDF-102 [12]. In this case the three codes: AMPX, TART and VIM literally interpreted the data according to the rules in ENDF-102, whereas NJOY used a different set of rules to produce the MCNP-Bob results. ENDF-102 defines a strict set of interpolation rules that do not work well with the $S(\alpha,\beta)$ model. In contrast MCNP-Bob rules are based on the actual $S(\alpha,\beta)$ model, and as such should be physically more acceptable.

Hopefully this example illustrates why I call the nuclear data processing codes the weak link that is often overlooked in our system of codes. In this case it seems clear that if all of the codes are to uniquely interpret the $S(\alpha,\beta)$ data, we must change either the ENDF-102 rules to be based on the actual $S(\alpha,\beta)$ model, or the evaluations in ENDF/B format to conform to the ENDF-102 strict interpolation rules – or both.

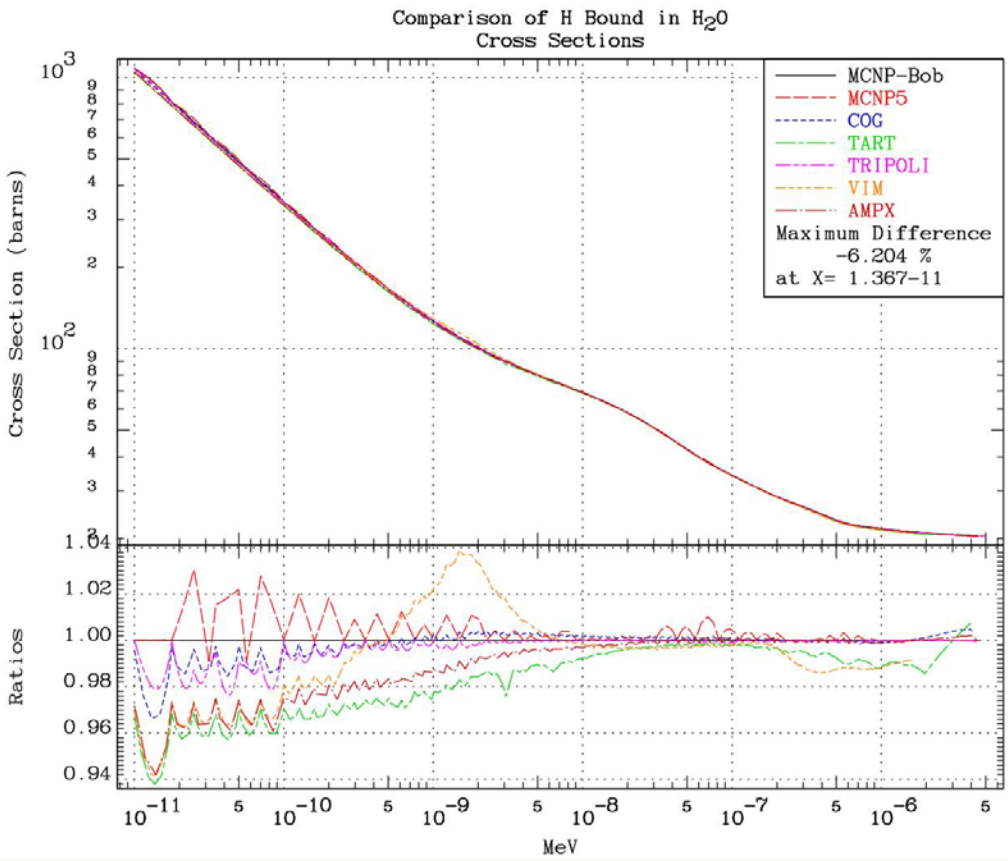

The scallops seen in the above plot are the result of each code using a different energy grid for its cross section. For a convex cross section generally using fewer energy points will cause scallops pointing upward, as in the case of the MCNP5 ratios at low energies in the above plot; using more energy points will cause scallops pointing downward, as in the case of the AMPX, TART and VIM ratios at low energy.

Because NJOY is so widely used to process nuclear data, below we present a plot of the cross sections produced by NJOY and used by a variety of codes, including: MCNP-Bob, MCNP5 (same as MCNPX) and TRIPOLI. All of these codes start with the same ENDF/B-VI thermal scattering law data, and all use the same nuclear data processing code, NJOY, and yet we still see differences of up to over 3% in the cross sections. Most of these differences are at lower energy, which is not that important, but we do see 1% between MCNP-Bob and MCNP5 near the peak of the thermal spectrum.

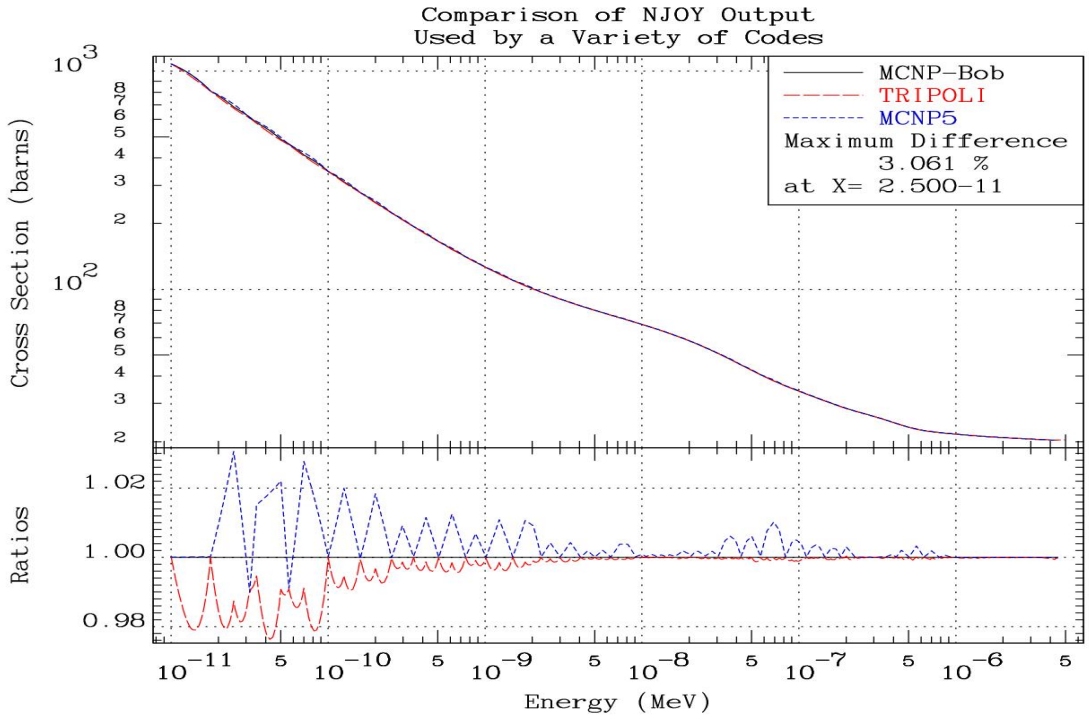

As mentioned earlier, the scallops on these plots are due to the use of different energy grids. Based on the above plot it appears that we are using the wrong code as the standard to ratio everything else to, as we will see below.

These three codes use quite different numbers of tabulated energy points to define the bound cross section: TRIPOLI 366 energy points, MCNP-Bob 106, and MCNP5 58. Of the three codes obviously TRIPOLI uses more energy points than the other two, and we can see this when we use TRIPOLI as the standard and ratio the others to it. Here we see upwards scallops for the other two codes, up to over 4%; for MCNP5 the bottoms of the scallops are at a ratio of 1.0, indicating agreement at common energies; in contrast MCNP5-Bob is somewhat higher.

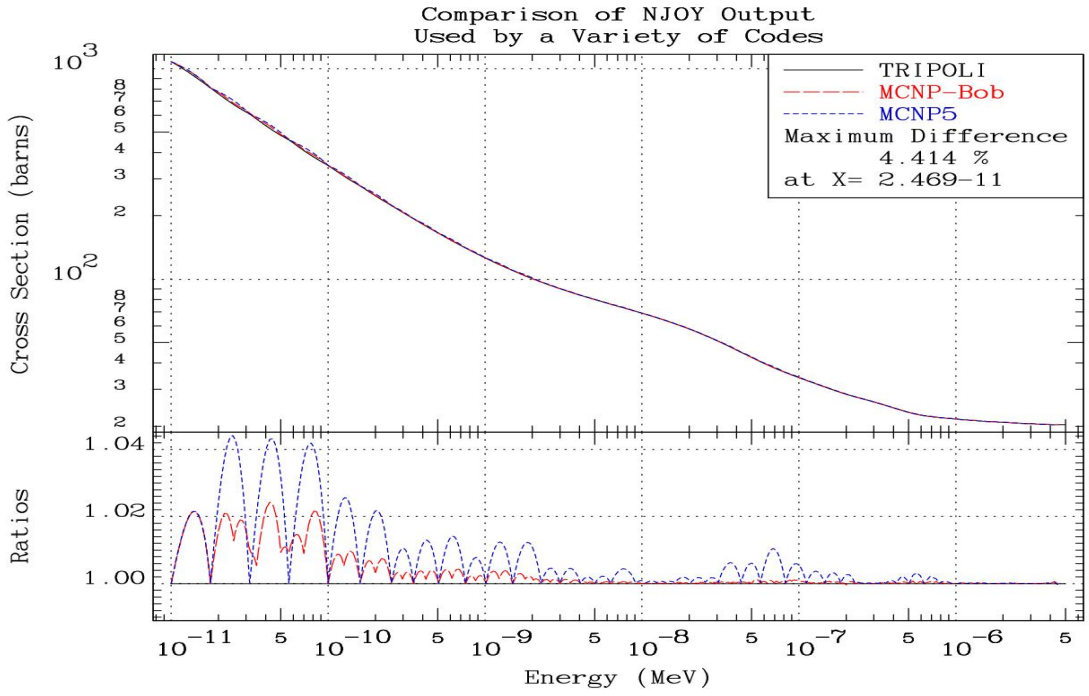

This is an excellent example of a processing code "dial" that can affect results, as mentioned in the introduction; here it appears that the TRIPOLI cross sections are based on the user telling the NJOY nuclear data processing code to produce many more energy points.

Let us reiterate that the differences we see in the above plots are completely due to the nuclear data processor codes used, and yet these are the some of the best codes available anywhere in the world. Please do not interpret our remarks concerning nuclear data processing codes in a negative sense. What the results presented here demonstrate is that not enough attention and resources are devoted to these codes. Again, let me stress: the results of any code can only be as good as the data it is using, so do not take nuclear data processing codes for granted; make every attempt to insure that the data coming out of your nuclear data processing code is as accurate as possible.

Besides the scatter cross sections, we also need scattered neutron secondary angular and energy distributions. When we examine these we see a real problem as far as making the bound and free atom scattering models consistent. As a reminder, we use bound data below some energy and free data at higher energy; for water the join energy at about 4 eV. This means that at all energies up to 4 eV we will use bound cross sections, as well as bound angular and energy distribution. Abruptly at the join energy and higher we will use free cross sections, as well as free angular and energy distributions.

Above we have already seen that we have a problem for the cross sections because these are not continuous at the join energy. Now let's look at the scattered energy spectra. It is claimed that for water the room temperature (293.6 K) bound spectra are similar to a free spectra at 1368 K, rather than a free spectra at 293.6 K. Therefore below we show all three. The first plot shows that below the incident neutron energy near 4 eV the bound spectra is similar to free at 1368 K, and very different from the free 293.6 K. But the second plot shows that above the incident energy the bound is similar to free at 293.6 K, and very different from 1368 K, i.e., neither free spectra agrees at all secondary energies. **The real problem is the peak in the bound spectra near the incident energy**. This peak does not appear in the free spectra at any temperature. Since this peak in the bound spectra is very persistent and extends to high incident energy, this features makes it impossible to smoothly join bound and free models at any energy.

The bottom line is that there is no energy at which we can smoothly join these spectra to make the bound and free models consistent. Nonetheless our codes do this, so our real question is: from a practical viewpoint how much does this inconsistency affect our calculated results?

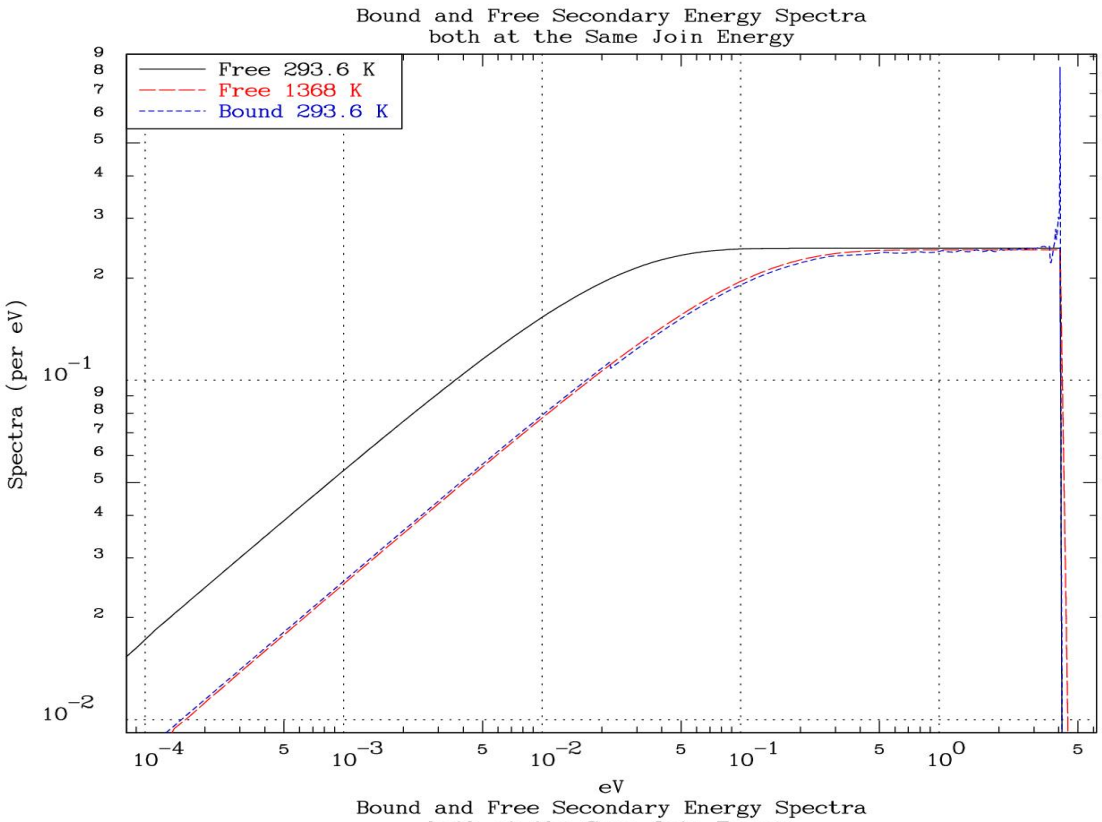
Bound and Free Secondary Energy Spectra
both at the Same Join Energy
Free 293.6 K
Free 1368 K
Bound 293.6 K
Spectra (per eV)
eV

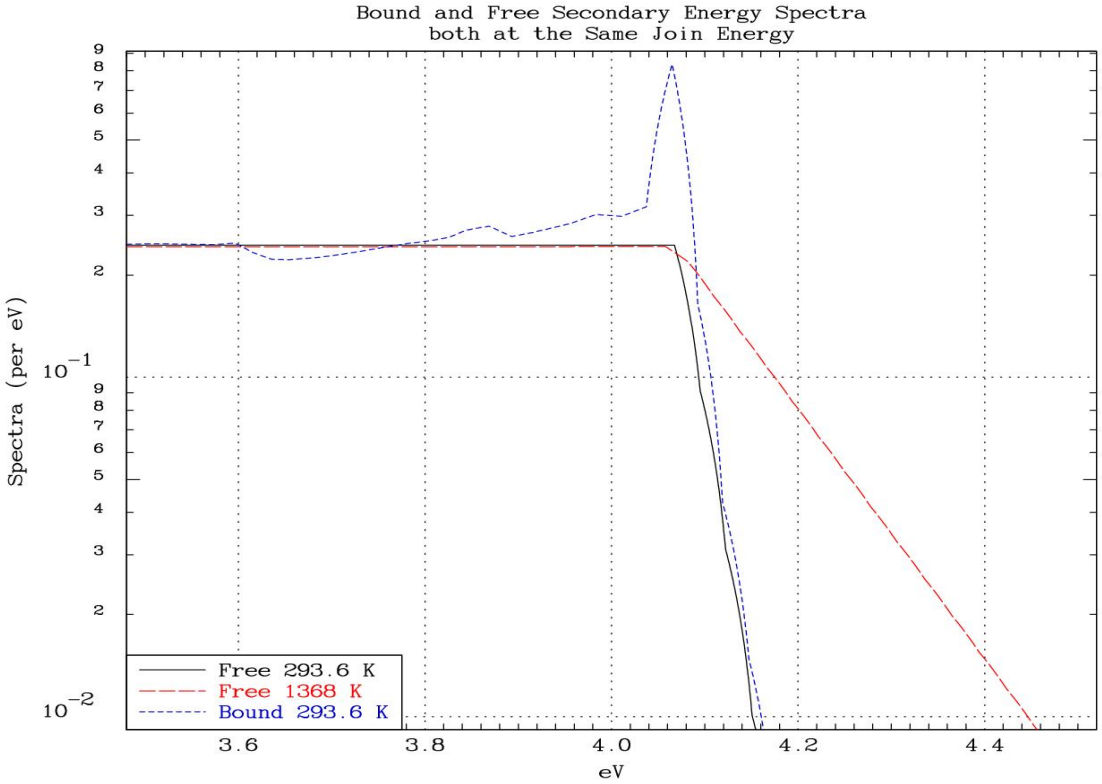
Bound and Free Secondary Energy Spectra
both at the Same Join Energy
Free 293.6 K
Free 1368 K
Bound 293.6 K
Spectra (per eV)
eV

Comparison to Experiments

The ultimate test of any model, such as the thermal scattering law S(α, β) model, is how well it agrees with experimental measurements, i.e. how does it compare to reality.

So far this report has addressed three very important issues: data processing, errors in codes, and the models that is used to define the thermal data, i.e., S(α, β) mode and free atom scatter. Hopefully, in the near future everyone will agree to use the same rules for processing the data and all will agree, and many of the coding errors will have been discovered and fixed. After those milestones are accomplished, the last one should be addressed: How well does the S(α, β) model cross sections agree with experimentally determined values.

If the measurements are correct and we use those data there is some hope that we will be able to successfully calculate the multitude of critical assemblies that we now have at our disposal for code and data verification. Having all the codes use the same data, processed the same way, to the same accuracy is a necessary first step, and clearly everyone is happy to discover and repair errors in their code, but the third step is just as important if we are going to predict the safety of systems for which experimental data are unavailable. Below is an overview of experimental data retrieved from the National Nuclear Data Center. The MCNP-Bob water cross sections are arbitrarily used for comparison; as we see above, other sets are similar. Note the cross section at 10^{-10} MeV is about twice the experimental value, which may not be significant in many problems because of the absence of flux at that such low energy, but nonetheless it indicates a problem with the S(α, β) model.

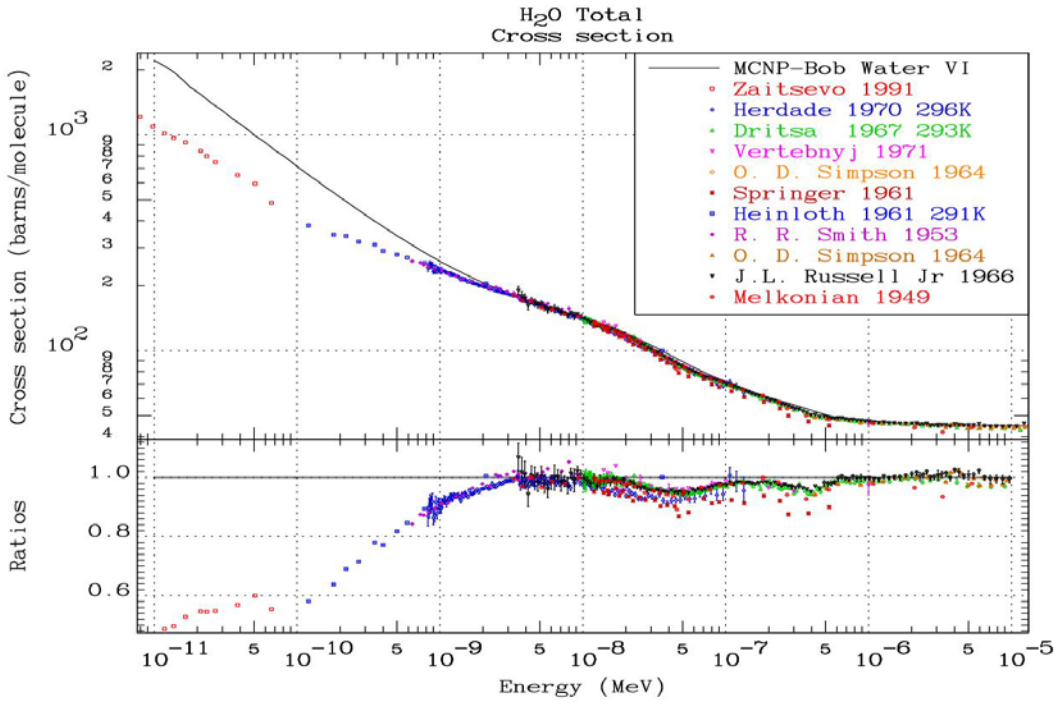

The scale of the figure above does not show any significant differences except at the lower energies. For the figure below the energy range was reduced in order to better show the differences of the ENDFB-VI, Rev.8 data (MCNP-Bob) from the experimental data. This report contains many examples to 2 to 5 percent differences due to problems discussed earlier; the figure below shows the same size differences that occur in the high flux region of thermal reactors or critical assemblies. For example, near room temperature thermal (0.0253 eV; 2.53 x 10^{-8} MeV) we see a number of experimental measurements that agree quite well, and none of them agree with the S(α, β) results, e.g., we see differences exceeding 6%.

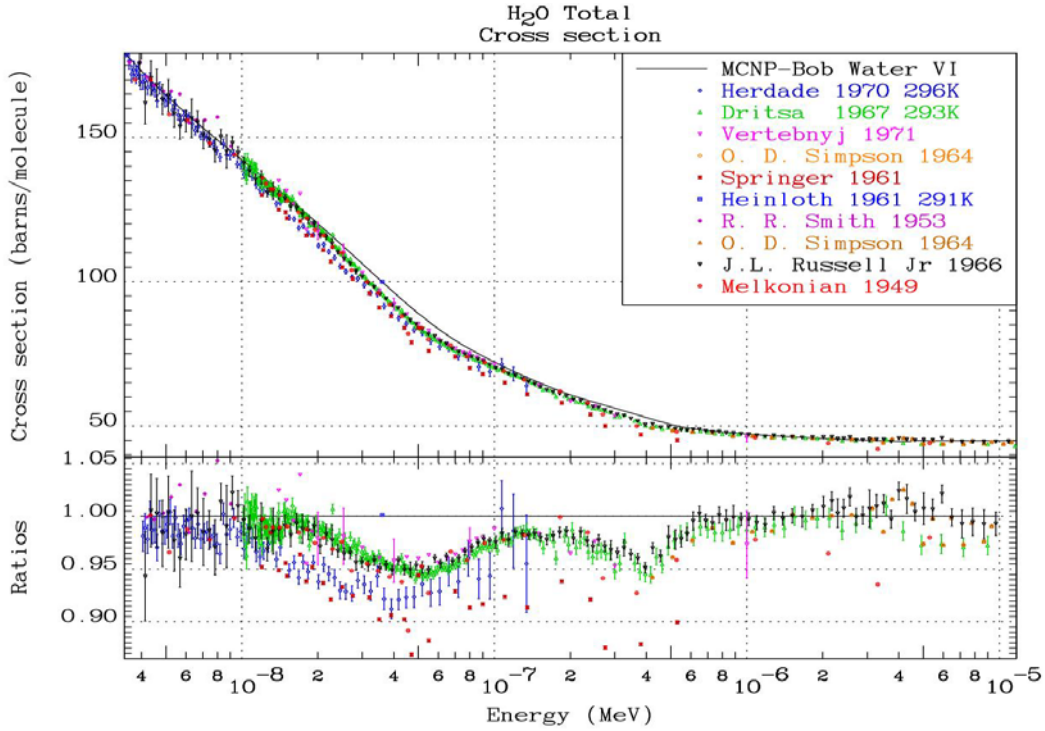

It is clear that the experimental data should be used if we are to be successful in calculating thermal critical assemblies. Models are great when they can be verified by experimental data, but the experimental data should not be ignored and replaced by model calculations, particularly if the two do not agree.

What these comparisons to experimental measurements indicate is that even after we have eliminated all differences between the cross sections produced by nuclear data processing codes, and all differences between the results produced by Monte Carlo transport codes, the S(α, β) model will still limit our ability to reproduce experimentally measured results.

Example Results: What is Important and what is not Important

Below we show an example flux spectrum within the water sphere and the leakage from the surface of the sphere. Here both quantities are normalized per source neutron, or if you prefer per neutron per second (quantitatively identical). The flux is the flux integrated over the entire volume of the sphere, and the leakage is the surface current integrated over the entire surface of the sphere. The integral of the leakage tells us that about 39.75% (0.3975 as a fraction) of the source neutrons leak from the system. There is no neutron production (fission, n,2n, etc.) within the sphere, so that by conservation the remainder 60.25% of the 14.1 MeV source neutrons are absorbed within the sphere.

The flux and leakage have similar shapes, but from the ratio we can see that with decreasing energy the ratio is decreasing, as the water cross sections increase thereby decreasing the leakage. By very low energy the water cross sections are so large that there is little leakage, e.g., on this figure, below about 10^{-9} MeV the leakage is just statistical noise.

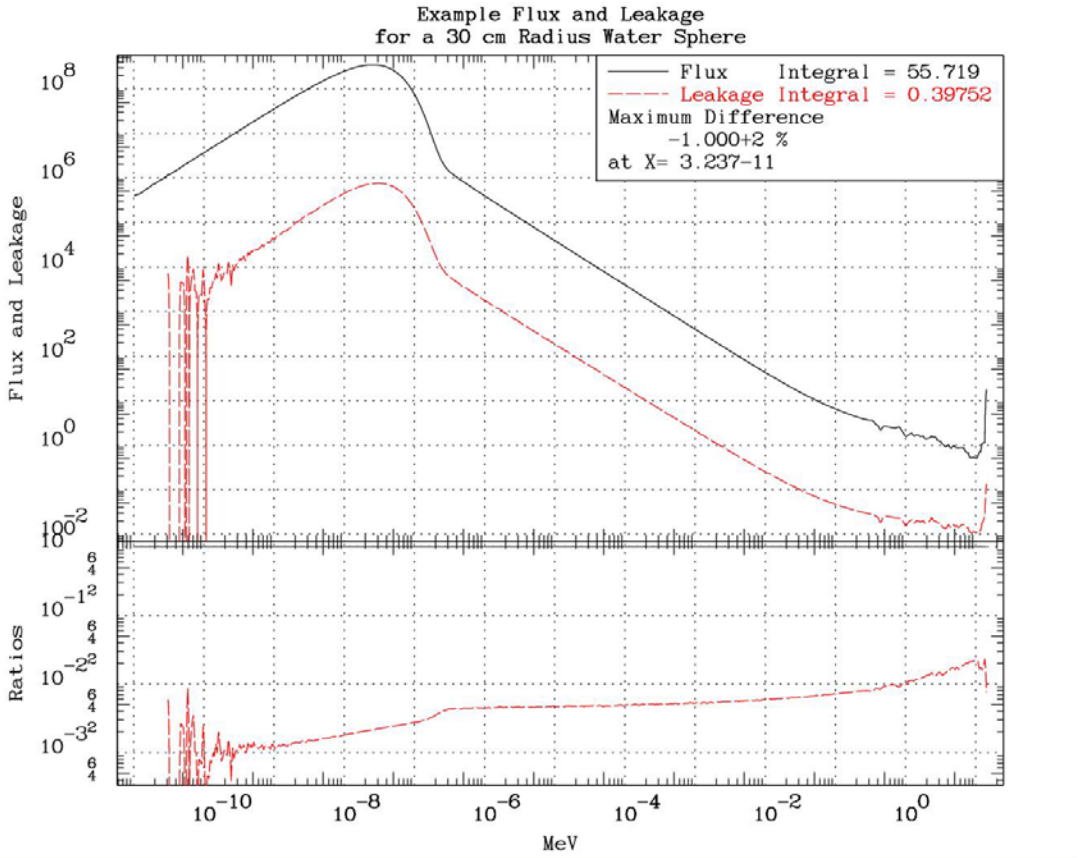

By integrating and normalizing each integral to unity we can see what energy ranges are and are not important, in terms of there contributing to the flux and current. Below we show these integrals first using log form and then linear form. Starting from the high energy at the 14.1 MeV source we can see a great deal of leakage near the source energy, both because of the low water cross sections and because the neutrons at the origin all start out pointing directly at the surface of the sphere. By 10 MeV we can see that 40% of the leakage has already occurred (60% remain), and by 1 MeV 75% (25% remain). There is then a slow gradual change in the integrals down to about 0.1 eV, and then an abrupt drop by 0.01 eV. From the log form we see can that below 0.001 eV there is very little flux or leakage, e.g., by 10^{-9} MeV the integral of the flux is only about 0.03% of the total, and the leakage is even smaller at about 0.005%; by 10^{-10} MeV, these are both roughly 2 orders of magnitude lower.

From these changes we can see that in terms of modeling changes in the flux and leakage, the energy range near the source is very important, as is the thermal range; in both there are relatively rapid changes in flux and leakage. From about 1 MeV down to 1 eV the integrals are very smooth and should be easy to model. The range below 0.001 eV (10^{-9} MeV) is of little or no interest, and we can ignore it in our comparisons, i.e., we expect only statistical noise at lower energies.

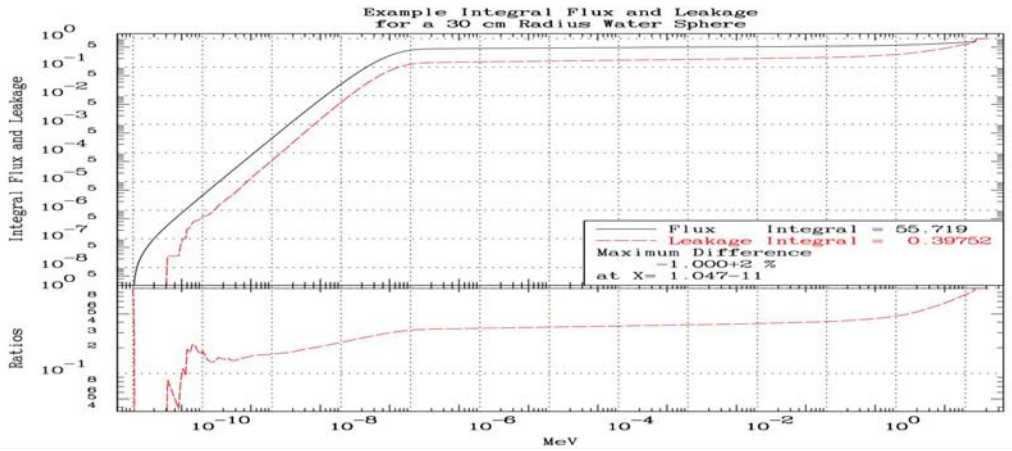

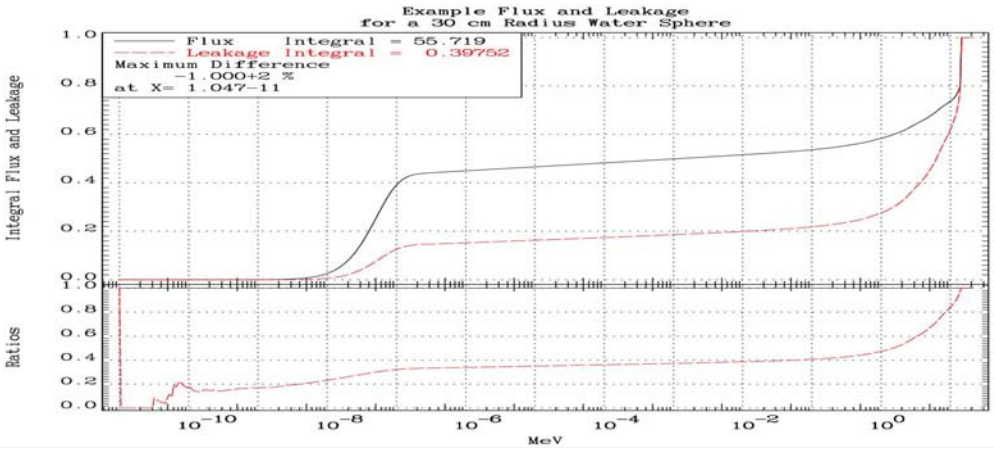
Example Flux and Leakage
for a 30 cm Radius Water Sphere
Flux Integral = 55.719
Leakage Integral = 0.39752
Maximum Difference
-1.000+2 %
at X= 1.047-11
Integral Flux and Leakage
Ratios
MeV

What do we expect the Answers to look like?

The equation that all of these codes are solving is the time independent, linear Boltzmann equation,

$$\Omega * \nabla \Phi(E,\Omega,R) + \Sigma_t(E) * \Phi(E,\Omega,R) = T(E,R,\Omega) + S(E,R,\Omega)$$

$$T(E,R,\Omega) = \int\int \Sigma_s(E') * p(E',\Omega' \rightarrow E,\Omega) * \Phi(E',\Omega',R)\, dE' d\Omega'$$

$\Phi(E,\Omega,R)$	= neutron flux
$\Sigma_t(E)$	= total macroscopic cross section
$\Sigma_s(E)$	= secondary macroscopic cross section
$p(E',\Omega' \rightarrow E,\Omega)$	= normalized secondary distribution
$T(E,R,\Omega)$	= secondary neutron distribution
$S(E,R,\Omega)$	= neutron source distribution

If we integrate this equation over all space and directions to have,

$$L(E) * \Phi_0(E) + <\Sigma_t(E)> * \Phi_0(E) = \int <\Sigma_s(E')> * p(E' \rightarrow E) * \Phi_0(E') dE' + S_0(E)$$

For convenience here we indicate leakage (L) as some multiple of the flux. If we further integrate over energy we find system integrated values,

$$<L> * \Phi_0 + <\Sigma_t> * \Phi_0 = <\Sigma_s> * \Phi_0 + S_0$$
$$<L> * \Phi_0 + [<\Sigma s> + <\Sigma a>] * \Phi_0 = <\Sigma_s> * \Phi_0 + S_0$$
$$<L> * \Phi_0 + <\Sigma a> * \Phi_0 = S_0$$

This is a basic conservation equation for our system. It states that for a steady state (time independent) solution, we have a **secular equilibrium**, where each second we add S_0 source neutrons to the system (the right hand side of this equation), which MUST be exactly balanced by the same number of neutrons per second being removed from the system by leakage and absorption (the left hand side of this equation).

Returning to our equation integrated only over space and direction, in our problem leakage is quite small and we can combine the first two terms as an equivalent total cross section times the flux. In addition in our problem the neutron source is monoenergetic, at 14.1 MeV, so it will be zero except at this energy. Considering these points we can simplify our equation to,

$$<\Sigma_t(E)> * \Phi_0(E) = \int <\Sigma_s(E')> * p(E' \rightarrow E) * \Phi_0(E') dE'$$

If we define the total reaction rate, $R_0(E) = <\Sigma_t(E)> * \Phi_0(E)$, our equation is,

$$R_0(E) = \int <C(E')> * p(E' \rightarrow E) * R_0(E')dE'; \quad C(E') = \text{secondaries/collision}$$

This is a simple balance equation which says that in order to have a steady-state, time independent solution, we must have equality between the total reactions causing neutrons to leave each energy E (the left hand side of this equation) and the scattering reactions causing neutrons to arrive at each energy E (the right hand side of this equation), remembering of course that this requires a time independent source of neutrons in order to have a non-zero solution.

This is the equation that we are solving at all energies. The main difference between higher and thermal energies, is that at higher energies scatter causes all neutrons to slow down in energy, i.e., $p(E' \rightarrow E) = 0$, for $E' < E$; whereas in the thermal range scatter can cause neutrons to either lose or gain energy.

From this equation we can see that any uniform change in cross section will be compensated by a similar but opposite change in the flux, such that the product, the **total reaction rate**, $R_0(E)$ remains constant, e.g., cross sections do not even appear in our equation defining the total reaction rate; for details of scaling see [13].

In the slowing down energy range we expect the solution to be 1/E in shape, and in the thermal range we expect it to be Maxwellian-like. Either one of these shapes can be modified by cross section scaling, e.g., in the slowing down energy range we expect the well known self-shielded solution, $\Phi_0(E) \sim 1/[E*\Sigma_t(E)]$. In the thermal range we expect the neutron density, n(E), to assume a Maxwellian shape, and since this is related to the flux by,

$$\Phi_0(E) = v*n(E) = v*\text{Maxwellian} \sim E*\text{Exp}[-E/T]$$

The figures below compare this prediction to our free results using a Maxwellian at 293.6 K, and our bound results using a Maxwellian at a slightly higher temperature to account from hardening due to binding. We can see that this prediction is excellent at defining both low energy limits (E variation) and it works well all the way up in energy to about the peak of the thermal spectra; beyond this point the spectra rapidly deviates from a Maxwellian shape as it becomes dominated by the 1/E slowing down spectra.

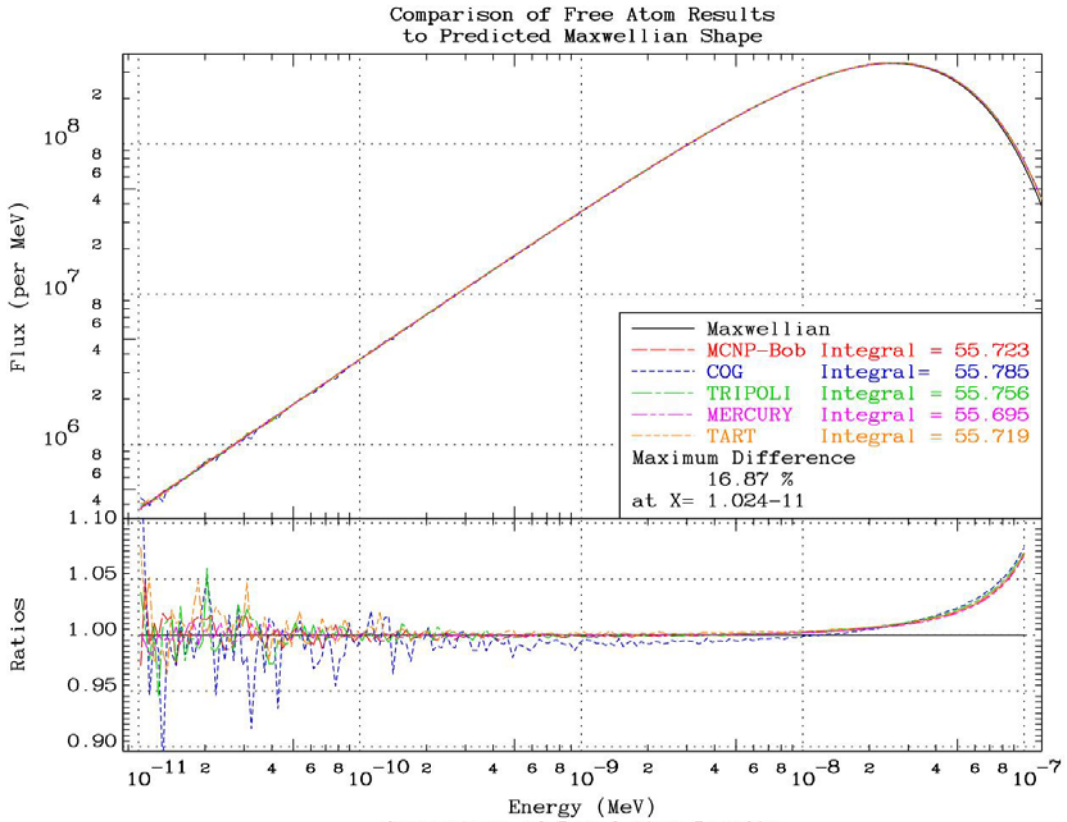
Comparison of Free Atom Results
to Predicted Maxwellian Shape
Flux (per MeV)
Maxwellian
MCNP-Bob Integral = 55.723
COG Integral= 55.785
TRIPOLI Integral = 55.756
MERCURY Integral = 55.695
TART Integral = 55.719
Maximum Difference
16.87 %
at X= 1.024-11
Ratios
Energy (MeV)

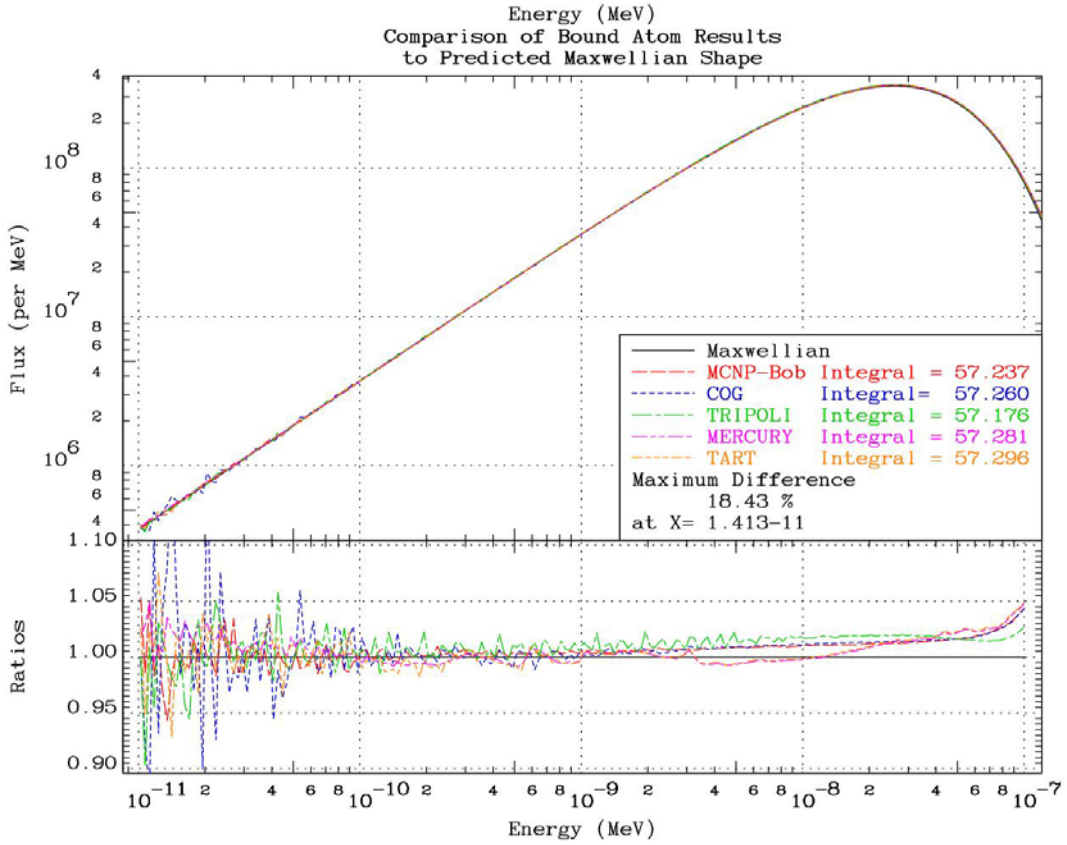
Comparison of Bound Atom Results
to Predicted Maxwellian Shape
Flux (per MeV)
Maxwellian
MCNP-Bob Integral = 57.237
COG Integral= 57.260
TRIPOLI Integral = 57.176
MERCURY Integral = 57.281
TART Integral = 57.296
Maximum Difference
18.43 %
at X= 1.413-11
Ratios
Energy (MeV)

One important point that we can learn from our definition of the **total reaction rate** is that it predicts that any change in the total cross section will be compensated by a change in the flux in the opposite direction. Since we will be comparing fluxes in this report, we should also expect to see an effect of a discontinuity of the cross section, as at the bound to free model join energy.

Background on Participating Neutron Transport Codes

All of the codes that we have results for are modern Monte Carlo transport codes. For the final round of comparisons all used the same ENDF/B-VI cross sections, so we need not worry about differences due to cross sections. All use continuous energy cross sections, so we need not worry about multi-group effects. All exactly modeled the simple spherical geometry, as a single sphere 30 cm in radius and filled with water at a density of 1 gram/cc. All started with the same 14.1 MeV monoenergetic neutron, point source at the origin of the sphere. All codes tracked the neutrons down to the lower energy limit of the ENDF/B cross sections at 10^{-11} MeV (10^{-5} eV).

In an attempt to minimize statistical noise in the answers, all used at least 100 million (10^{8}) source neutrons; TART and MERCURY used 1,000 million (10^{9}). This reduces the statistical uncertainty over most of the energy range to a small fraction of 1%. Even with this many source neutrons we still see statistical noise near the lower end of the energy range, where the above plots show the integral effect on flux and leakage is extremely small, i.e., the probability of a Monte Carlo code transporting neutrons to this energy range is extremely small.

What effects are we interested in?

Ideally we would like to demonstrate that all participating codes get the same answer; here we only investigate the scalar flux inside the water sphere. Beyond this, if we do find differences we would like to understand the sources of differences, so that we can eliminate them. In the water system that we studied a primary concern is correctly modeling neutron scatter.

In our transport codes we use up to three different models of neutron scattering in different energy ranges. Starting at high energy we use a **stationary target** scattering model, where we assume the atoms in the material are stationary and the moving neutrons interact with these atoms with the relative speed of the neutron. At somewhat lower energies, in the keV – eV energy range, we use a **free atom** scattering model, where we assume the atoms in the material are randomly moving about in a Maxwellian distribution corresponding to the local temperature; here the relative speed is defining by the vector combined speed of a neutron and an atom of the material. Both of these models are approximations that used in combination with evaluated neutron angular distributions allow analytical calculation of the

neutron secondary energy and direction. Finally at still lower energy, in the eV and below energy range, we use a **bound atom** scattering model, the thermal scattering law data, where we assume that rather than being free, the atoms are bound in a molecule, e.g., here we are interested in H1 bound in H2O. Here no analytical solution is available, and we must use the S(α, β) model, which involves tabulated data to approximate the distribution of secondary neutrons in energy and direction; currently this is the only thermal scattering model available in evaluated nuclear data files, such as ENDF/B.

The codes use somewhat arbitrary discrete energies at which they switch from one scattering model to another. One of our primary concerns is consistency of these three models used together in our calculations, e.g., do the results of one model smoothly transition to the results of the next model as a neutron transports down in energy, and if not how large an effect do we see.

Below we will find that although each code uses a different energy to switch from stationary atom to free atom, we do not see any significant effect on the calculated flux. For example, for the case using only **free atom data**, the flux calculated by all of the codes agree quite well.

Unfortunately, this is not the case when the codes switch from free to bound atom as the neutrons slow down in energy. Here we find discontinuities in the scattering cross sections and in the spectra of secondary energies of scattered neutrons. Keeping in mind that all three of these scattering models are only MODELS (approximations), the question is: are these inconsistencies of any importance, as far as affecting differential quantities such as flux, and integral quantities such as reactivity. Below we attempt to answer this question.

Comparisons of Flux Results for Monte Carlo Codes

Below we compare results separately for the cases using **free atom** and **bound atom** cross sections. Here we present results for only one of the family of MCNP codes, namely MCNP-Bob. In the next section we present results for all three codes in this family: MCNP-Bob, MCNP5 and MCNPX.

First we present results from five Monte Carlo codes: MCNP-Bob, COG, MERCURY, TRIPOLI and TART. As on the figure above we arbitrarily use a MCNP-Bob as a standard and ratio everything else to it. This does not mean that we consider MCNP-Bob to be better, or worse, than any of the other codes; it is merely convenient so that we can quantitatively see the magnitude of the differences between the results.

How can we judge results: Who is right or wrong?

Below we present the results as submitted by each of the codes compared to be results from all other codes, we point out where we see important differences, but

we do not try to go beyond this point and judge who is right or wrong. Unfortunately, in this study it was not possible for us to decide who is right or wrong. What you will see in the figure belows are results from seven different Monte Carlo codes, no two of which produce the same answers for the two cases using free and bound cross sections. This presents us with a problem similar to what we saw above, where we presented seven sets of cross of H1 bound in H2O scattering cross sections, no two of which agree. Unfortunately, in this study it was not possible for us to decide who is right or wrong.

All we can do is show the magnitude of the differences from these codes. A lot of work still remains to be done before we can claim we really know “the right answers”. Even though today we do not know the answers, this study has contributed significantly toward understanding the sources of differences, which will aid us in being able to eliminate these differences.

Free Atom Scattering Results

The figure below shows an overview of the entire energy range from 10^{-11} MeV to 15 MeV. On this scale we see generally good agreement over the entire energy range, except at very low energy where we see the expected statistical noise, but we also see differences in the MeV energy range.

Note that even though we see significant differences in the energy dependent flux, the integrals of the flux over energy are very similar, in the narrow range 55.705 to 55.756; a variation of only 0.041, or about 0.07%.

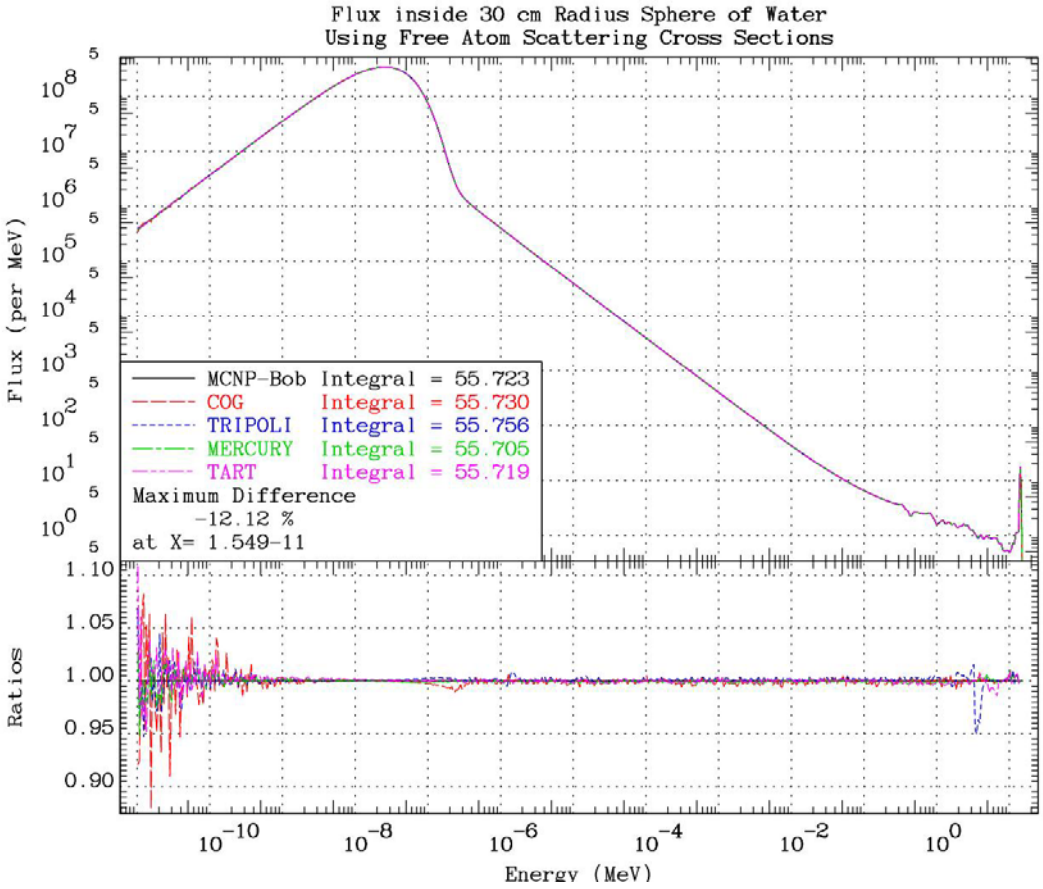

The figure below is the same as the figure above, except that the statistically insignificant energy range below 10^{-9} MeV has been deleted. Here we more clearly see the differences. If you first focus only on the upper part of this figure, you will see what appears to be excellent agreement between all of the codes, e.g., they all appear to agree within the thickness of the lines. Only by looking at the ratios in the lower part of this plot can we quantitatively see differences of up to 5%. Surprisingly the biggest differences of up to 5% is in the MeV energy range, but at low energy, near an eV, we also see differences of about 1%.

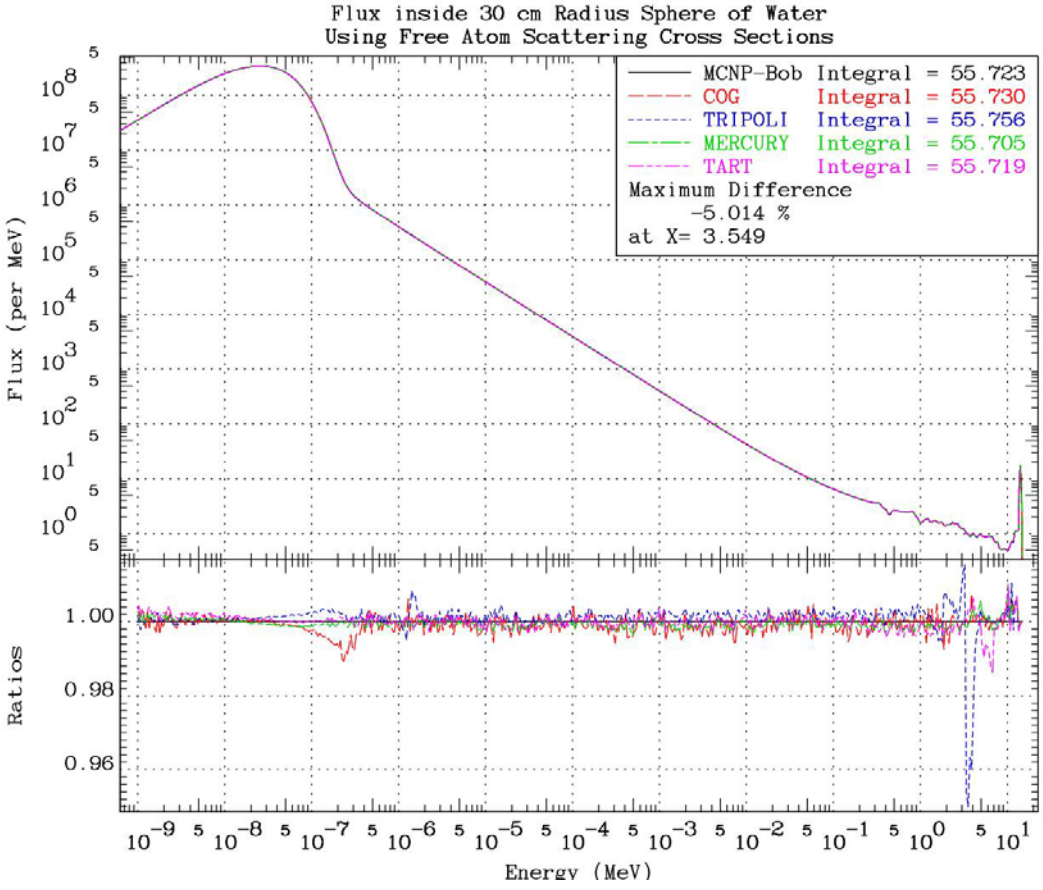

The following sequence of figures starts at the 14.1 MeV neutron source energy, and shows progressively lower energy ranges that the neutron slow down through. The figure below shows a detail of the 1 to 15 MeV range. Here we see generally good agreement, except for: a 5% difference for TRIPOLI in the 3 to 4 MeV range, and 1% differences for TART in the 5 to 7 MeV range.

Because of the system we are modeling this turned out to be a particularly difficult energy range. The spike that we see at high energy is due to the 14.1 monoenergetic source. The spectrum from 14.1 down to about 10 MeV is due to elastic scattering from hydrogen and oxygen; the lowest inelastic level is at about 6 MeV, so that inelastic scatter cannot contribute to the flux in this energy range. Below about 8 MeV we see the combined effects of elastic and inelastic scatter down to about 6 MeV. Below this point only elastic scatter occurs. What was particularly difficult to model was the angular distribution of the oxygen elastic scatter that defines the shape of the flux between 14.1 and 8 MeV. Our initial comparisons showed up to 80% differences in this energy range. These were traced to errors in codes (this was the source of the biggest differences), and to a lesser degree differences in cross sections. Only after code errors were eliminated and everyone agreed to use the same nuclear data were we able to reduce the differences to those shown below.

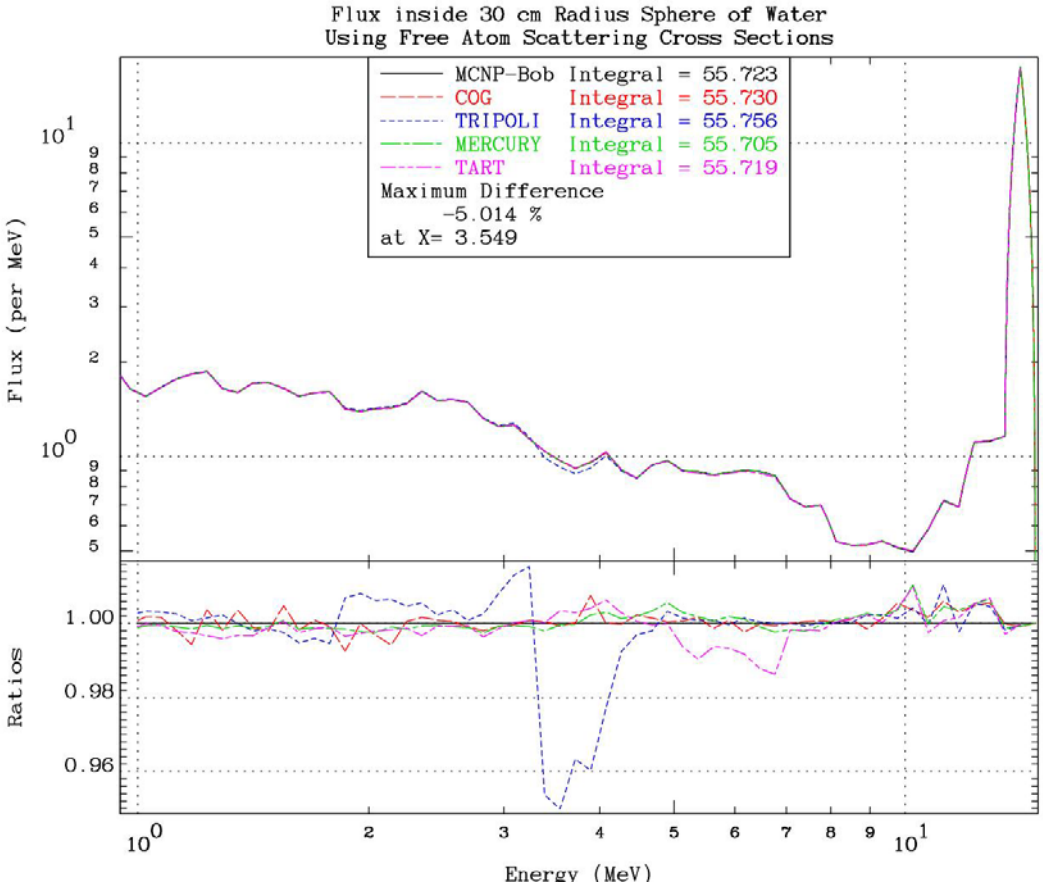

The figure below shows a detail of the slowing down energy range from 1 MeV down to 1 eV. Here we see outstanding agreement between all five codes with only statistical differences at the 0.1% to 0.2% level.

This is a particularly important energy range, and for our system it should be trivial for us to calculate, since all that is involved is elastic scattering of H and O. As shown above, even systems as different as uranium pin cell in water and the simple water sphere used in this study have the same basically 1/E slowing down spectra, all the way from close to the MeV range, down to the eV, where the flux feeds into the thermal spectra. As such any error in this energy range will have a direct effect on what happens at lower energies in the thermal range, e.g., a 1% error in normalization here will translate into a 1% error in the thermal range. Our initial comparisons showed up to 10% differences in this energy range. These were traced to errors in codes (this was the source of the biggest differences), and to a lesser degree differences in cross sections. Only after code errors were eliminated and everyone agreed to use the same nuclear data were we able to reduce the differences to those shown below.

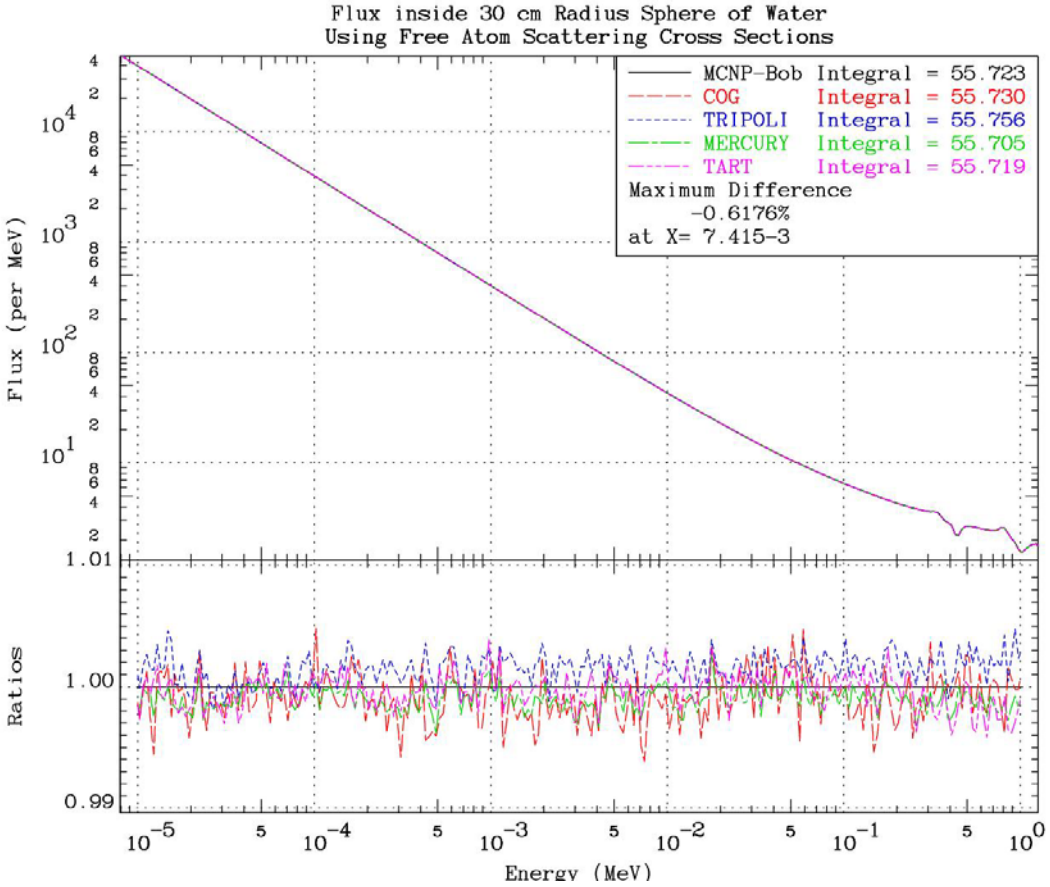

The figure below shows a detail of the 1 milli-eV to 10 eV range (10^{-9} to 10^{-5} MeV). Here we still see very godd agreement between the codes with only statistical differences at the 0.1% to 0.2% level, except for a few narrow energy ranges, where we see differences up to 1%.

For a water cooled thermal reactor this of course is where most of the reactions happen (see, reference [1] for details), so it is extremely important that we be able to accurately calculate results here. Our initial comparisons showed up to 10% differences in this energy range, which were traced to problems in the slowing down normalization. Only after code errors were eliminated and everyone agreed to use the same nuclear data were we able to reduce the differences to those shown below.

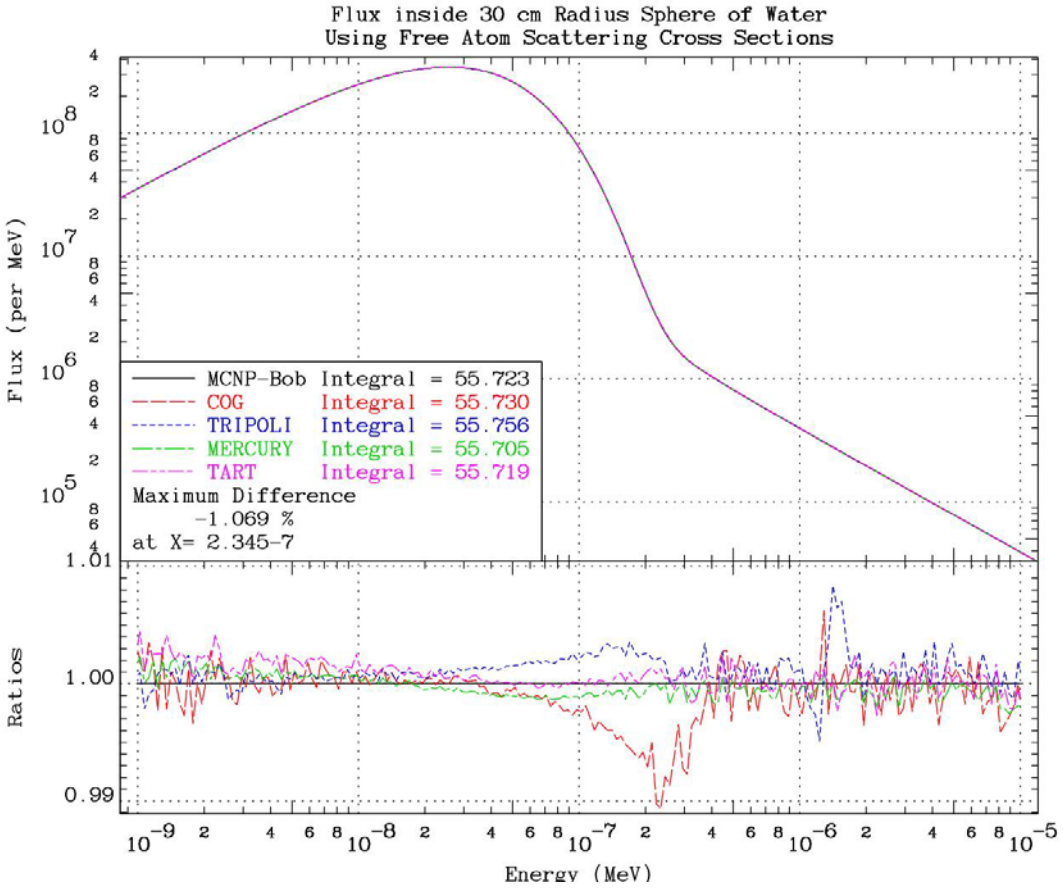

As mentioned above, log scaling can often mask the real magnitude of differences, so below we show the important energy range around the peak of the thermal spectrum. Note that near the peak of the spectrum all of the codes agree very well at the 0.2% level; this indicates that for integral values, such as the reaction rates, even though the energy dependent fluxes differ, all of these codes will produce similar integral results.

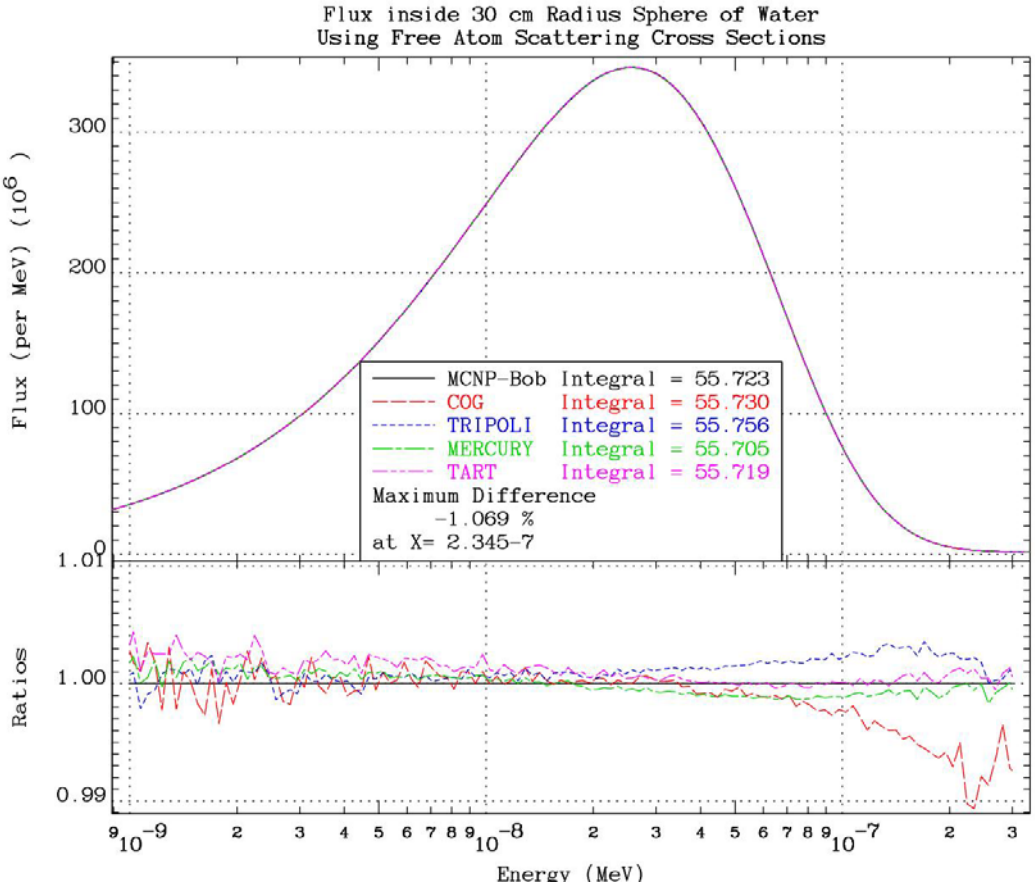

Bound Atom Scattering Results

The figure below shows an overview of the entire energy range from 10^{-11} MeV to 15 MeV. Above about 4 eV these results are as expected identical to the free atom results. At very lower energy we see the expected statistical noise. Also below 4 eV we see significant differences.

Note that even though we see significant differences in the energy dependent flux, the integrals of the flux over energy are very similar, in the narrow range 57.176 to 57.296; a variation of only 0.120, or about 0.21%.

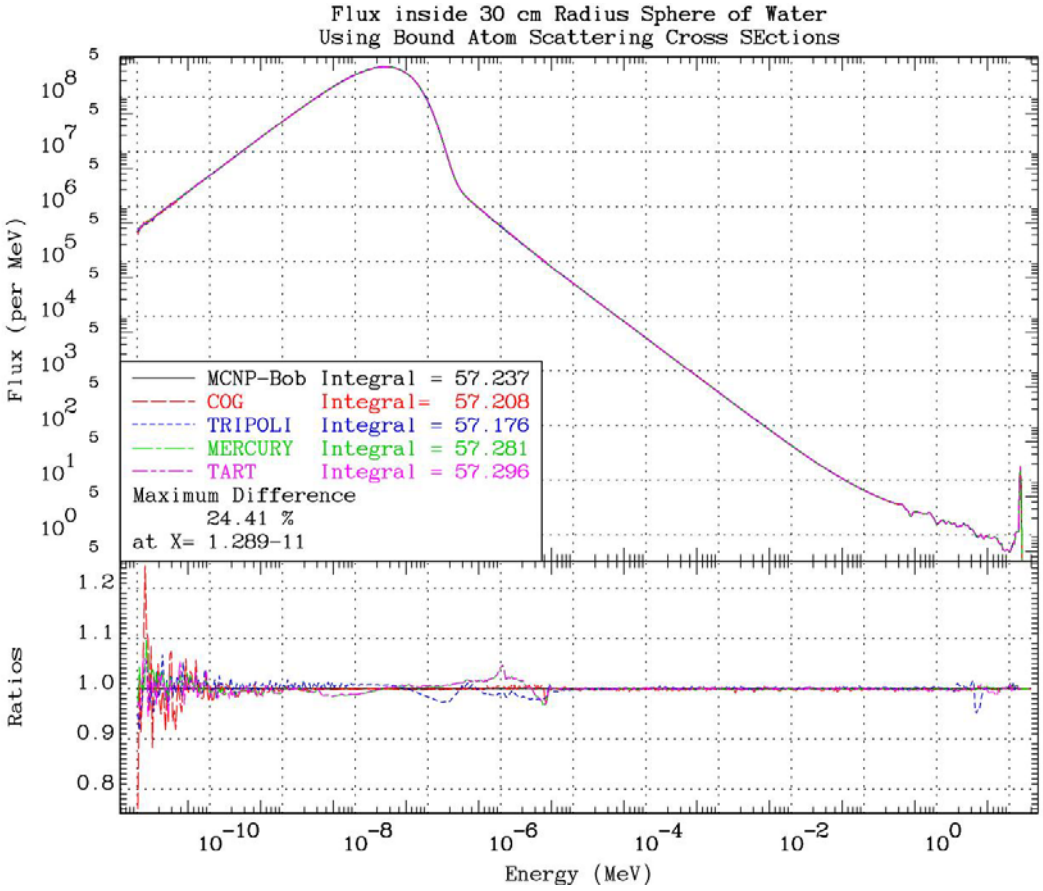

The figure below is the same as the figure above, except that the statistically insignificant energy range below 10^{-9} MeV has been deleted. Here we more clearly see the differences. Since the results above 4 eV are the same as the free atom results presented above we need only examine the results below this energy.

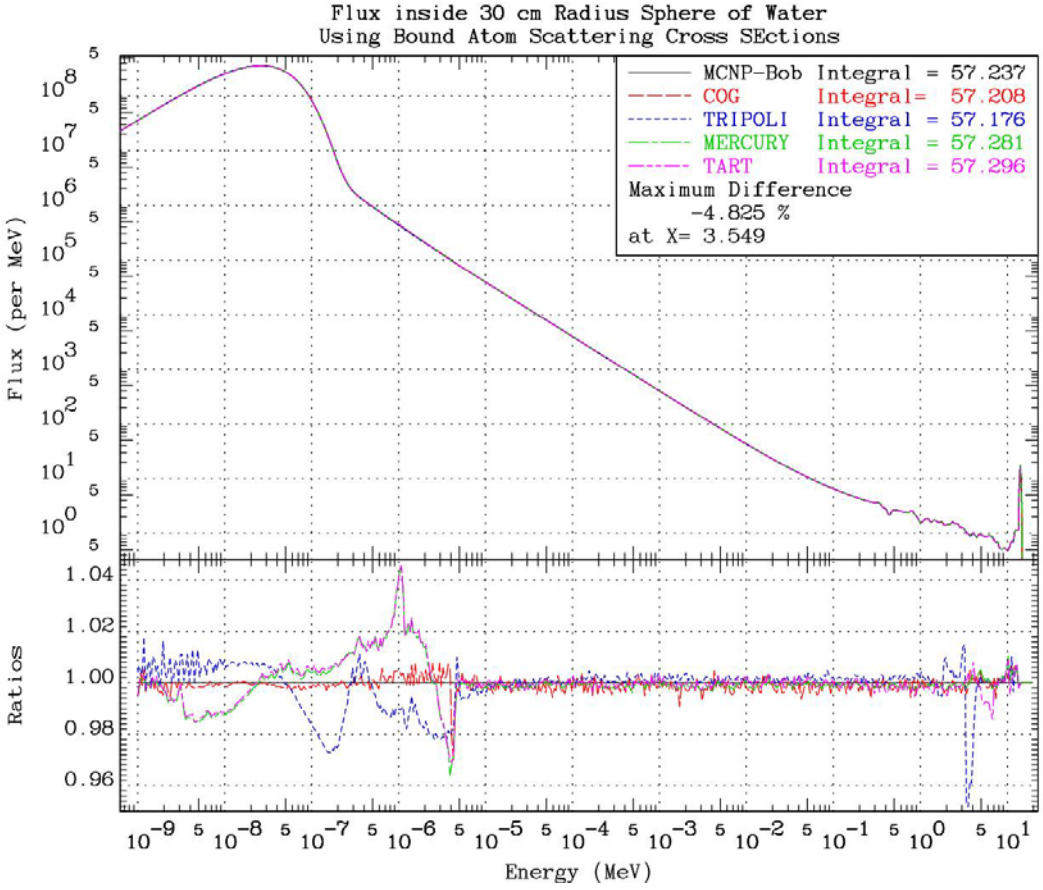

The figure below shows the detailed energy from 1 milli-eV up to 10 eV (10^{-9} to 10^{-5} MeV). Here we can see the differences in the calculated flux due to how each code handles the bound thermal scattering law data. Note in particular the differences we see in the 1 to 4 MeV energy range of up to +/-4% for MERCURY and TART; more about this below.

From this figure we can see that below 4 eV, MCNP-Bob and COG agree very closely, as do TART and MERCURY. These pairing are not surprising since MCNP-Bob and COG are interpreting the S(α, β) data according to one set of rules, and TART and MERCURY are interpreting the same data according to a different set of rules. We can see that this results in differences in the scalar flux of up to +/-4%.

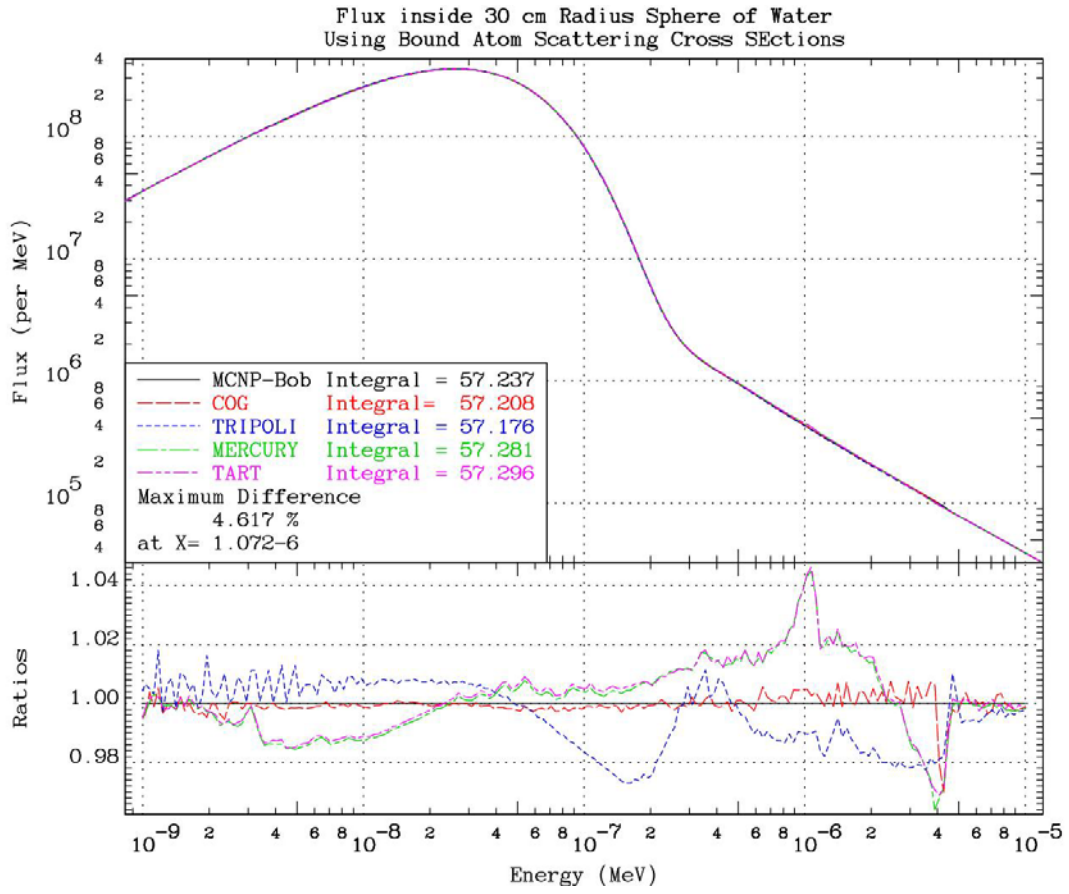

Overall the agreement is very good. If we look only at the upper part of these figures it is hard to see any differences at all (to within the thickness of the lines). Only the lower part of these figures showing the ratios allows us to find the per-cent differences. Again, remember that the small differences seen here were achieved only after several iterations to improve the agreement between code results.

Physically nothing changes in neutron scattering where we join the free and bound scattering models. This tells us that if the bound and free atom models are consistent, the slowing down flux based on free atom scattering should smoothly pass through the join energy between our models and then continue on to lower energy using our bound atom model; this does not assume either model is correct, only that they are consistent. Therefore any anomalous effects that we see at or near the join energy are due to inconsistencies between our models.

To judge whether or not we have a problem near the join energy, 4 to 5 eV, for the figure below we use the MCNP-Bob calculated free atom flux as a standard and we ratio everything else to it. Again, if the models are consistent we expect a smooth transition of the flux from free to bound energy range. What the figure below shows is that the discontinuities in the cross sections that we saw earlier, causes a jump in the flux. Remember that at the join point the MCNP-Bob, TRIPOLI and COG bound cross section is less than the free cross sections, so as they cross the join energy we see a corresponding jump upward in the flux, by up to about 3%.

In contrast the MERCURY and TART results, which use continuous cross sections, show the physically acceptable smooth transition through the join energy. However, even though these results look more physically acceptable, in order to make the cross sections continuous the TART cross sections were somewhat arbitrarily modified to force continuity, so that their results are no more reliable than that of the other codes where we see a discontinuity.

The bottom line here is that we cannot claim that near the join energy one of these results is any better, or worse, than any of the other results. All we can say is that based upon using one model or the other we see differences of about +/-4% near the join energy.

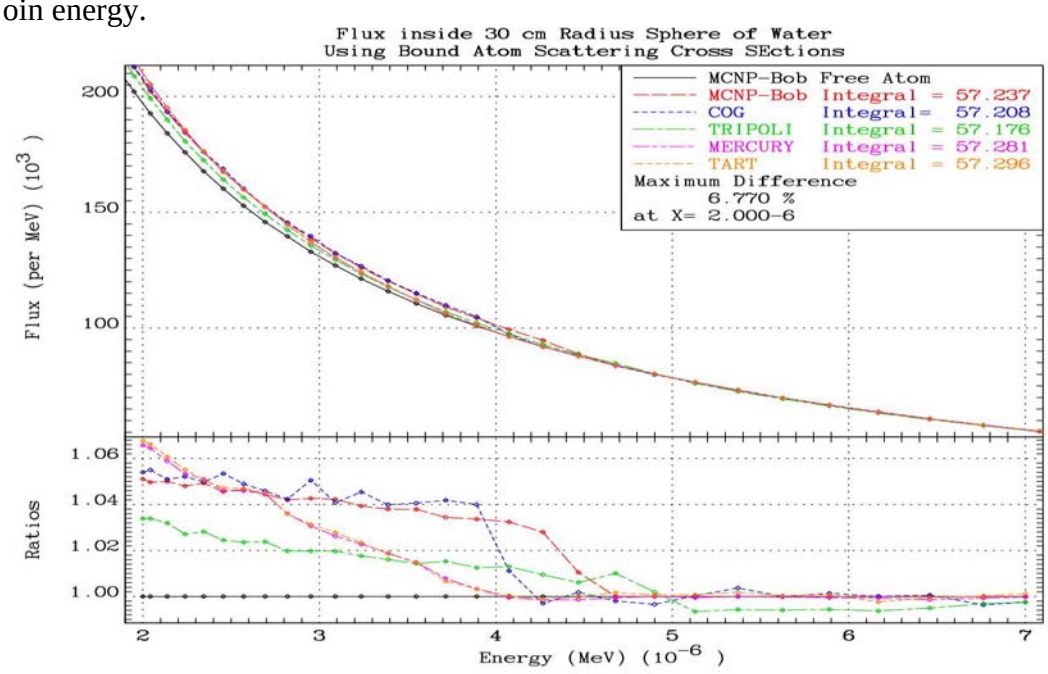

As mentioned above, log scaling can often mask the real magnitude of differences, so below we show the important energy range around the peak of the thermal spectrum. Note that near the peak of the spectrum all of the codes agree well at the 1% level. This agreement is not great, and certainly no where near as good using free atom, but it is much better than what one might expect by looking at a wider energy range.

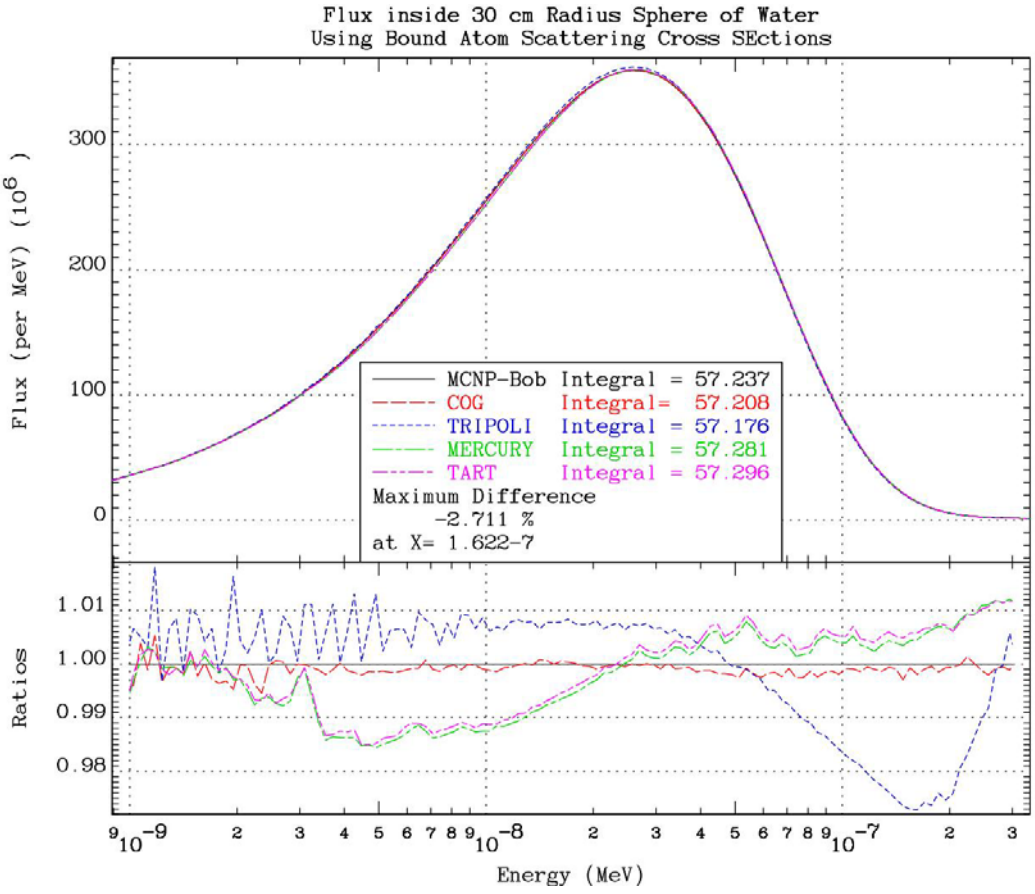

Comparisons of Results for the MCNP Family of Codes

Currently there are two different versions of MCNP available for general use, MCMP5 and MCNPX [4] both distributed by Los Alamos National Laboratory. In addition there is an yet unreleased version of the code that in this report we refer to as MCNP-Bob [5], since it is Bob MacFarlane who is primarily involved in its development. As related to our study of the slowing down of neutrons in water, the most important difference is the treatment of thermal scattering law data.

Briefly, the thermal scattering law data used by both MCNP5 and MCNPX is produced by the cross sections processing code NJOY [9]. Starting from ENDF/B-VI thermal scattering law data, NJOY processes it into the form of a number of discrete secondary energies and cosines. MCNP5 uses the data in exactly this form; we will see below that the result is a thermal scattering spectrum that rather than being continuous, includes a series of "spikes", each spike corresponding to one of the defined discrete (secondary energy, cosine) values. MCNPX starts from the same discrete data and being aware of the problem with MCNP5, attempts to smooth the spectrum by interpolating between the tabulated discrete values. This MCNPX procedure does produce a smoother spectrum than that produced by MCNP5, but it is still far from what MCNP-Bob produces. For use with MCNP-Bob, NJOY has been updated to produce continuous in secondary energy and cosine distributions that are smooth, much more physically acceptable, and now agrees with the spectra produced by the other codes that have participated in this comparison. Although it is not yet publicly available, it is planned that MCNP-Bob will be available in the not too distant future.

Our first plot compares the three codes using free atom cross sections. For this problem all three codes produce the same results; no problem here.

The results are quite different when we use bound thermal scattering law data. The first plots shows an overview of the entire energy range showing good agreement at higher energy, but obvious large differences at low energy.

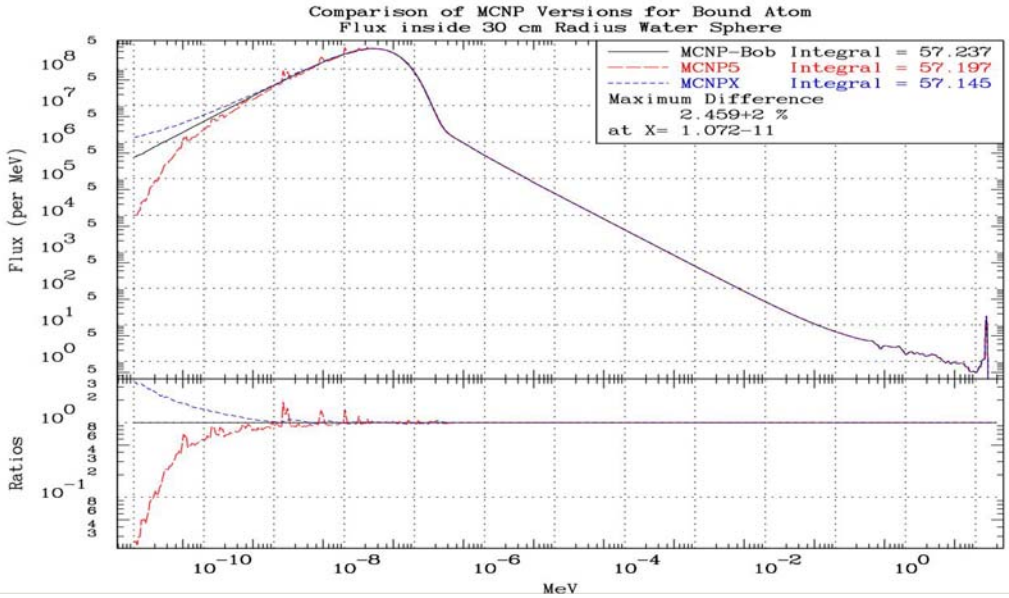

The second plot shows perfect agreement above 10 eV (10^{-5} MeV on the plot). Based on the perfect agreement that we saw earlier using free atom data, this is not surprising, since the bound data only extend up to 4 eV, and we expect the results using free and bound data to be identical above this energy.

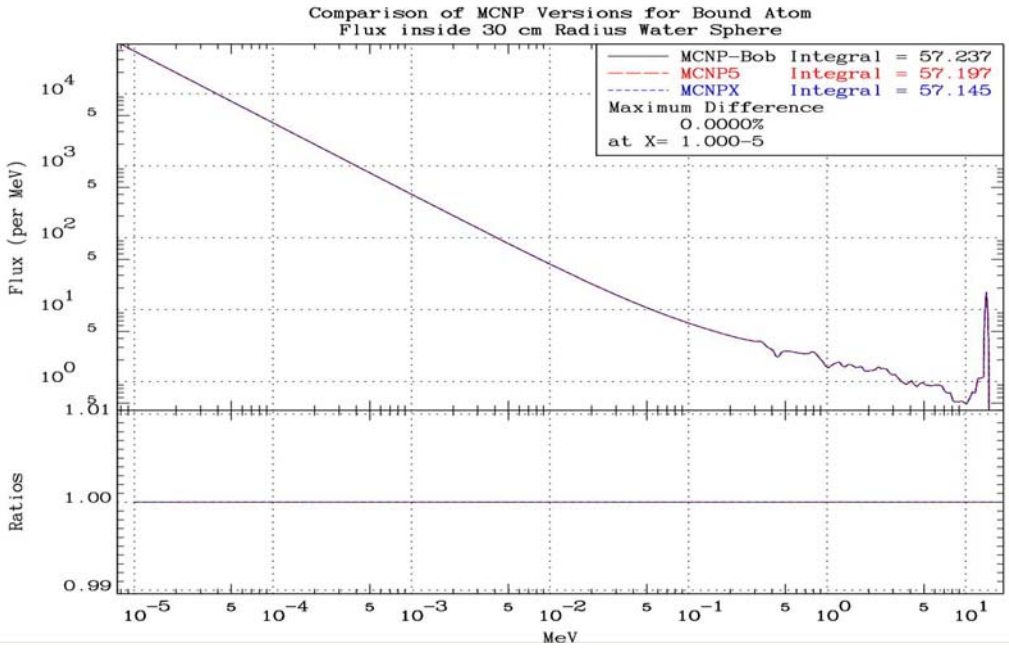

The third plot shows the important thermal energy range from 0.01 eV, below the peak of the thermal spectrum up to 10 eV. Here we can clearly see the affect on the MCNP5 spectrum of using discrete secondary energies (the red spikes on the figure). We can also see the affect on the MCNPX spectrum of trying to smooth the spectrum; this eliminates the MCNP5 spikes, but is still far from the MCNP-Bob results.

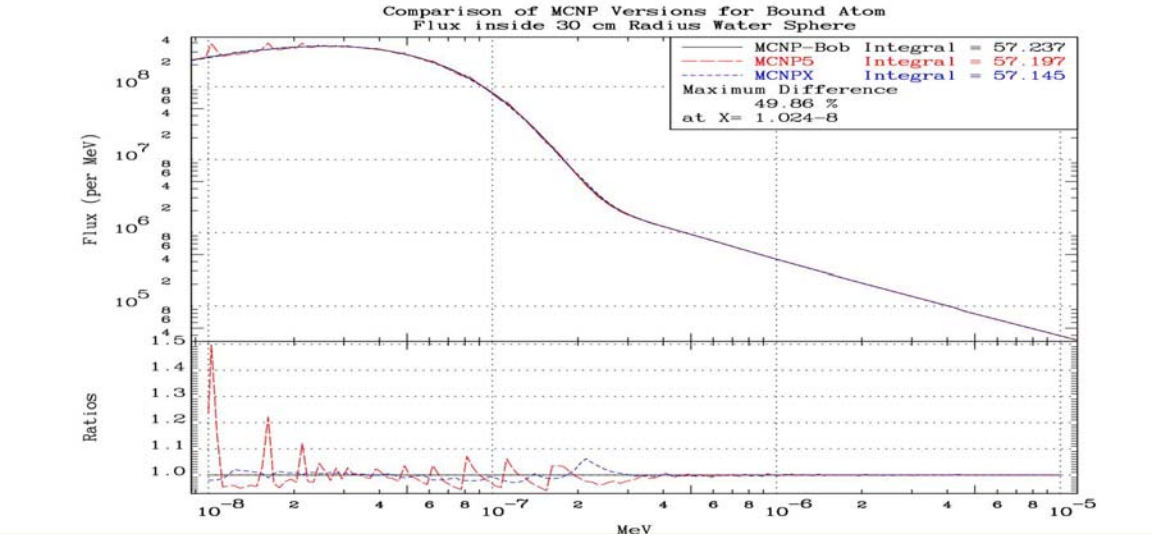

The fourth plot shows the results for the three codes deviating from one another at low energy. Whereas MCNP-Bob has the expected 1/E variation, MCNPX is higher than this, and MCNP5 is much lower than this. In fairness we should mention that in terms of integral effects the energy range below about 1 milli-eV (10^{-9} MeV on the plot) is of little importance; if we had truncated this figure at 1 milli-eV this effect would be hardly noticeable.

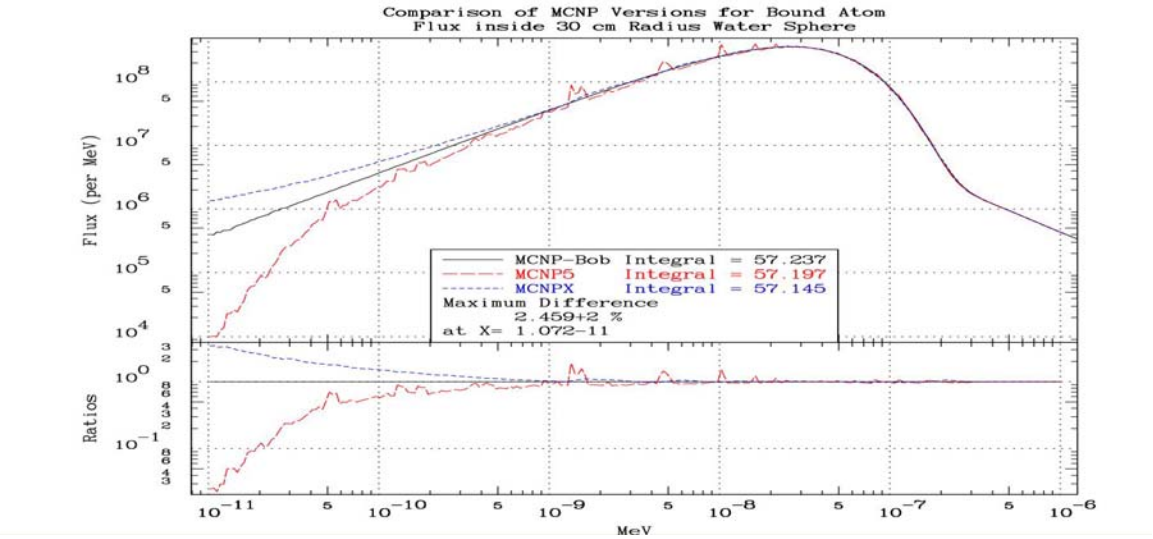

Sometimes it is difficult to judge the actual magnitude of differences on log scaled plots, so below we show a comparison of the spectra calculated by the three codes across the entire peak of the thermal spectrum. Here we can more clearly see the smoothing effect of MCNPX, and the spike of MCNP5. The second figure shows that MCNPX still differs from MCNP-Bob by a significant amount; not the factors of 2 seen for MCNP5, but still by up to 10%.

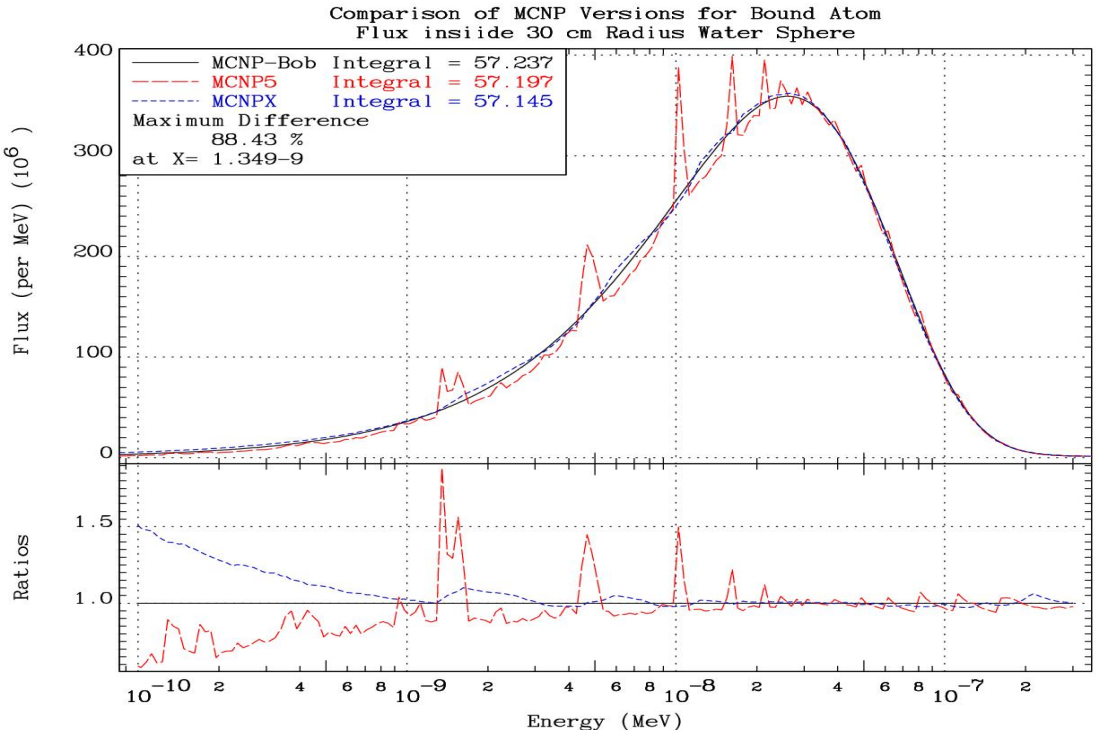

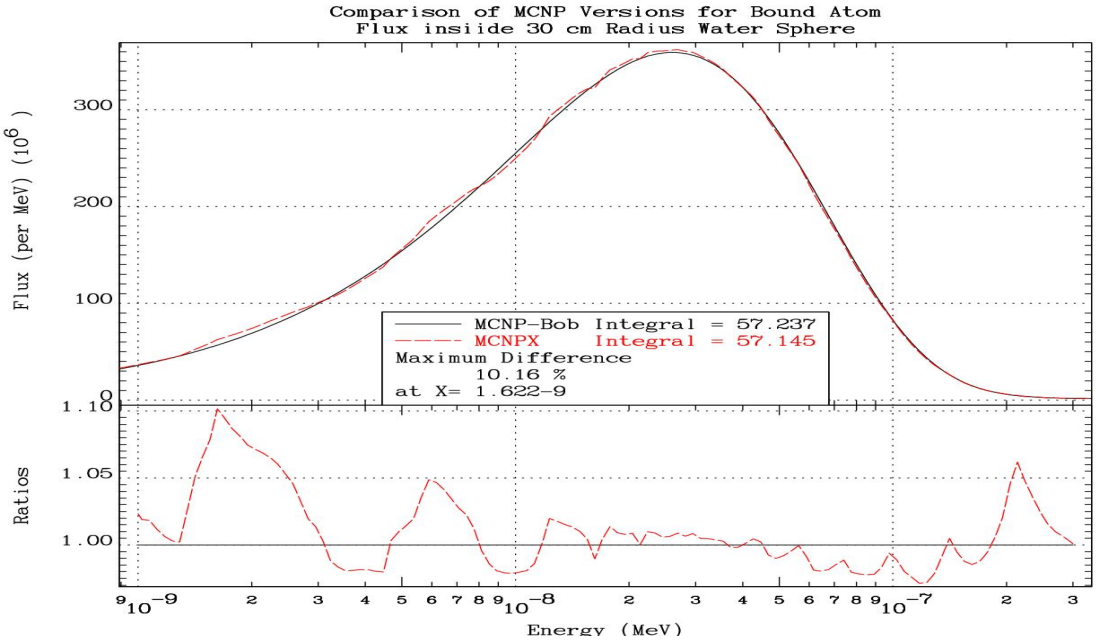

Prospects for the Future

All of the above results are based on what our codes can do today, using the ENDF/B-VI Thermal Scattering Law Data, S(α, β). The ENDF/B-VI data library has now been frozen, so there is nothing that we can do to improve it. However, the ENDF/B-VII library is now under development and preliminary S(α, β) data are now available; these data are quite similar, but not identical to JEFF-3.1 data. Here we look only at the water cross sections, again compared to available experimentally measured data, but now including both ENDF/B-VI and VII, preliminary cross sections. The ENDF/B-VI bound data extended up to 4.46 eV, whereas the ENDF/B-VII data extend up to 10 eV.

The first plot below shows that compared to the ENDF/B-VI cross sections, the preliminary ENDF/B-VII cross sections, agree better with the measurements at lower energy, e.g., the factor of two difference at low energy has been cut in half, to 50% difference, and the general agreement has been extended below 10^{-9} MeV (1 milli-eV).

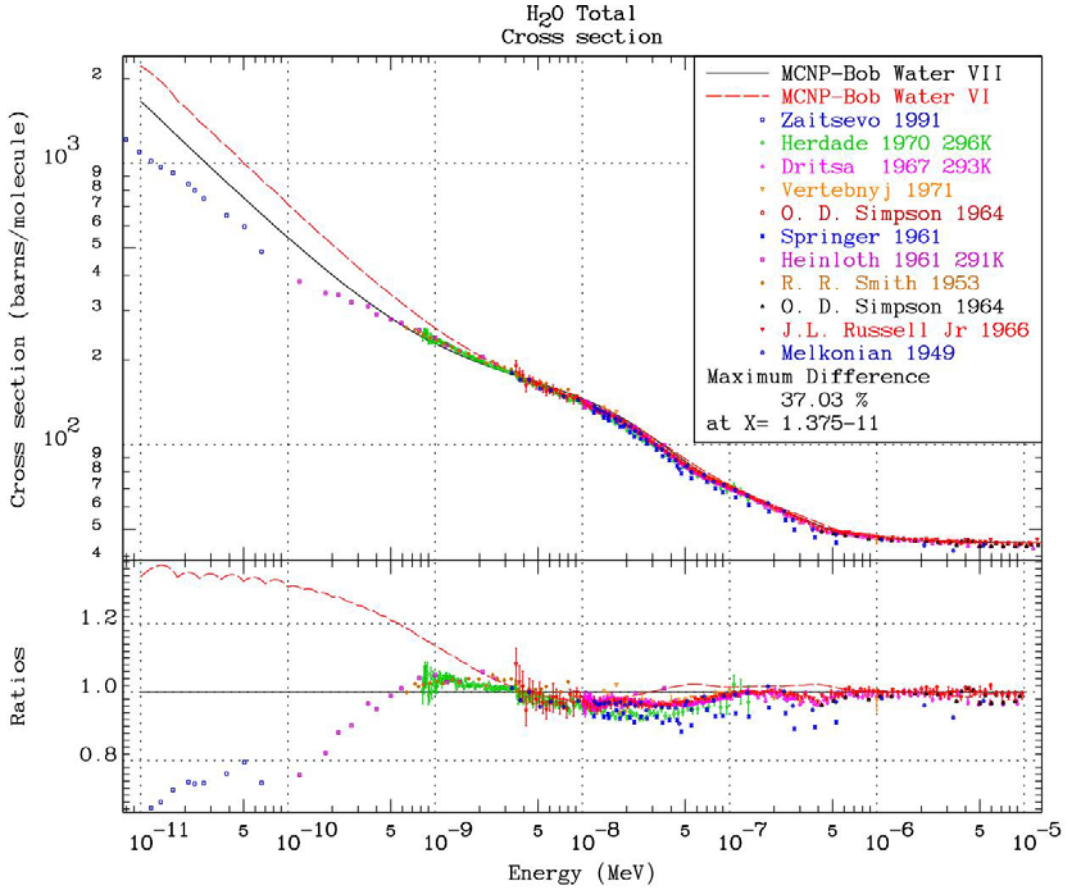

The figure below shows that the ENDF/B-VII cross sections are a few per-cent lower than the ENDF/B-VI cross sections over about a decade of energy from near thermal energy (0.0253 eV, 2.53 x 10^{-8} MeV) extending up toward 1 eV. Near thermal energy the ENDF/B-VI values were over 6% higher than the measurements; the ENDF/B-VII values are still about 3 to 4% higher than measurements. Due to the spread in the measured data, above about 1 eV it is difficult to decide whether bound or free atom cross sections are in better agreement with experiments.

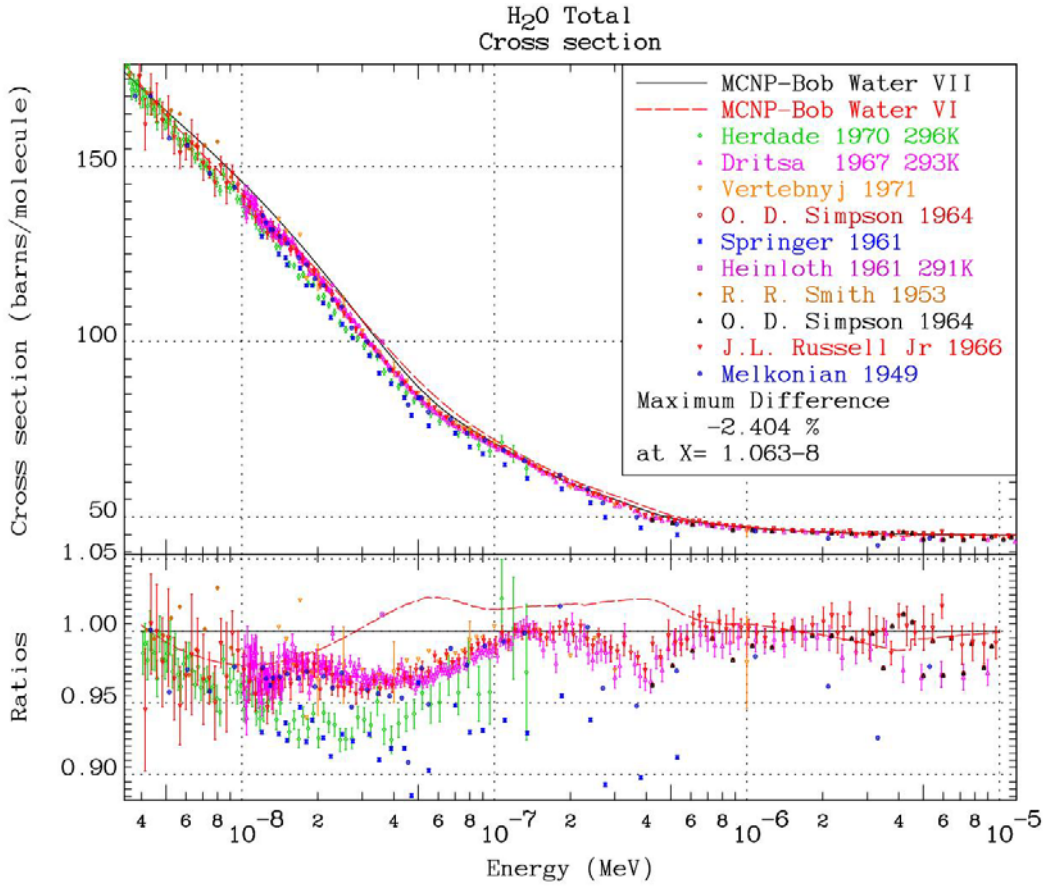

In summary we can see that the preliminary ENDF/B-VII cross sections are significantly different from ENDF/B-VI cross sections, and agree somewhat better with experimentally measured cross sections. But through the important thermal energy range they still differ by about 4% from measured values; note, near 0.0253 eV all of the measured values agree quite well and all are lower than the VI and VII cross sections. We must stress that the ENDF/B-VII cross sections shown here are only PRELIMINARY, and may change significantly before they are finalized for use in ENDF/B-VII.

The Importance of Code Comparisons

We feel that we cannot stress enough the importance of code comparisons. Today our codes are far to complicated to be able to assume that hard work and being conscientious are enough to produce error free codes. Experience has repeatedly demonstrated that only through code comparisons can we find the errors that exist in every code, and most importantly, only then are we in a position to eliminate these errors. In the case of this seemingly trivial study of the slowing down in water, **ALL of the participating codes were improved based on these code comparisons**.

Our experience has been that participation in code comparisons is a win-win situation, where you have everything to gain and nothing to lose by participating. Unfortunately, our experience has also been that it takes a lot of confidence for users to have the courage to show that they and their codes are not perfect. Unfortunately, many people do not have this confidence, which is what limits the number of codes that participate in our comparisons. That is truly unfortunate, since we always try to avoid embarrassing anyone, and all participating codes end up improved and verified for certain types of calculations.

Conclusions

We have compared the results produced by a variety of currently available Monte Carlo neutron transport codes for the relatively simple problem of a fast source of neutrons slowing down and thermalizing in water. Initial comparisons showed rather large differences in the calculated flux; up to 80% differences. By working together we iterated to improve the results by: 1) insuring that all codes were using the same data, 2) improving the models used by the codes, and 2) correcting errors in the codes; no code is perfect.

Even after a number of iterations we still found differences, demonstrating that our Monte Carlo and supporting codes are far from perfect; in particularly we found that the often overlooked nuclear data processing codes can be the weakest link in our systems of codes.

The results presented here represent the **today's state-of-the-art**, in the sense that all of the Monte Carlo codes are modern, widely available and used codes, using the most up-to-date nuclear data, and the results are very recent, weeks or at most a few months old; these are the results that current users of these codes should expect to obtain from them. As such, the accuracy and limitations of the codes presented here should serve as guidelines to code users in interpreting their results.

We avoid crystal ball gazing, in the sense that we limit the scope of this report to what is available to code users **today**, and we avoid predicting future improvements that may or may not actual come to pass. An exception that we make is in presenting results for an improved thermal scattering model currently being testing

using advanced versions of NJOY and MCNP that are not currently available to users, but are planned for release in the not too distant future. The other exception is to show comparisons between experimentally measured water cross sections and preliminary ENDF/B-VII thermal scattering law, S(α, β) data; although these data are strictly preliminary they are currently available and undergoing testing and these results were judged to be within the scope of this report.

During this study we found inconsistencies between our bound and free scattering models, as well as problems with the individual models, including,

1) Different interpretation of the S(α, β) model by our nuclear data processing codes resulting in differences in the bound scatter cross sections used by our Monte Carlo codes.
2) Discontinuity in the scatter cross section at the energy where bound and free models join.
3) Discontinuity in the energy spectra where the models join.
4) Differences between measured cross sections and those based on the S(α, β) model.

Of these 1) is currently being worked on and should be eliminated as a problem in the not too distant future. Even after all of the codes are using the same cross sections, the other three problems still remain.

So who is right and who is wrong? Unfortunately, from the results of this study we cannot answer this question, since no two codes that participated in this study agree on the answers. The only "absolute" standard that we have to compare to is the experimentally measured water cross sections. All we can do is report the magnitude of the differences we see between code results. More work needs to be done to understand and eliminate the differences we see here.

There is one positive conclusion that we can reach from this study: regardless of how much time and effort we put into improving our Monte Carlo codes, we are never going to eliminate differences unless we improve our nuclear data processing codes. How many times do we have to keep repeating the following: the results of any Monte Carlo code can be no better than the nuclear data it use. Our results here illustrate that the accuracy of these data are currently limited by what is being produced by nuclear data processing codes.

We hope that the results presented here serve as a wake up call to those who think our Monte Carlo codes systems and the nuclear data they use are "now perfect". The results presented here show the true state-of-the-art today, based on using the "best" available nuclear data, nuclear data processing codes, and Monte Carlo neutron transport codes. This should serve as a WARNING for current code system users as to how accurate and reliable the answers are from these codes. Today our codes are good – often very good – but far from perfect and it is important that code users understand this point and do not try to read into code results more accuracy than they can practically deliver. Be aware that there is more uncertainty in Monte Carlo answers than the estimates of statistical uncertainty printed out by the codes.

Today we have so much computer power available that we can run Monte Carlo codes long enough to reduce statistical uncertainty to such small values, that this become irrelevant as an estimate of the overall accuracy of results, which can be limits be other factors, such as the quality of the data your code is using.

References

[1] "How Accurately can we Calculate Thermal Systems", UCRL-TR-203892, Lawrence Livermore National Laboratory, by Dermott E. Cullen, et al., April 2004.; now available on-line at http://www.llnl.gov/cullen1/pin_cell.htm

[2] New Thermal Neutron Scattering Files for ENDF/B-VI Release 2, LA-12639-MS (ENDF 356), Los Alamos National Laboratory, by Robert E. MacFarlane, March 1994.

[3] **COG:** A Multiparticle Monte Carlo Transport Code, User's Manual, Fifth Edition, UCRL-TM-202590, Lawrence Livermore National Laboratory, by Richard M. Buck, Edward Lent, Tom Wilcox, Stella Hadjimarkos, September 1, 2002.

[4] **MCNP:** A General Monte Carlo N-Particle Transport Code, Version 5, Volume I: Overview and Theory, X-5 Monte Carlo Team, Los Alamos National Laboratory report LA-UR-03-1987, April 24, 2003. Portions of the MCNP manual on-line at http://www xdiv.lanl.gov/x5/MCNP/themanual.html

[5] **MCNP-Bob:** Bob MacFarlane has update his NJOY processing nuclear data processing for MCNP to produce continuous secondary energy distributions. The angular distributions are still discrete equally probable cosines as before. He has updated a version of the Monte Carlo code MCNP5 to sample from the continuous energy distributions. Angular sampling smears out the discrete cosines. It is this combination of NJOY-MCNP that we refer to in this report as MCNP-Bob. As yet this NJOY-MCNP combination is not available for general use.

[6] **MERCURY:** MERCURY User Guide (Version b.8), Lawrence Livermore National Laboratory, Report UCRL-TM-204296, Revision 1, by R. J. Procassini and J. M. Taylor, (2005), more information concerning MERCURY is available online at http://www.llnl.gov/mercury

[7] TART05: A Coupled Neutron-Photon 3-D, Combinatorial Geometry Time Dependent Monte Carlo Transport Code, UCRL-SM-218009, Lawrence Livermore National Laboratory, by Dermott E. Cullen, November 2005, available online at http://www.llnl.gov/cullen1/mc.htm

[8] **TRIPOLI-4.3** User Manual for version 4.3 of the TRIPOLI-4 Monte Carlo method particle transport computer code, CEA-R-6044, by J. P. Both, A. Mazzolo, O. Petit, Y. Peneliau, B. Roesslinger, CEA/Saclay, France, November 2003. TRIPOLI-4 version 4.3.2 is available from http://www.nea.fr/abs/html/nea-1716.html

[9] **NJOY:** "The NJOY Nuclear Data Processing System, Version 91," Los Alamos National Laboratory report LA-12740-M, by R. E. MacFarlane and D. W. Muir, (October 1994) is still the latest official manual.

[10] **AMPX:** "AMPX-2000: A Cross-Section Processing System for Generating Data for Criticality Safety Applications", TANSAO 86, p. 118, (2002), by M.E. Dunn and N.M. Greene,

[11] **VIM:** Status of the **VIM** Monte Carlo Neutron/Photon Transport Code, by R. N. Blomquist, Proceedings of the 12th Biennial RPSD Topical Meeting, Santa Fe, NM, April 14-18, 2002. Separate VIM User's Manual available with the code from RSICC.

[12] **ENDF-102:** Data Formats and Procedures for the Evaluated Nuclear Data File ENDF-6, ENDF-102; BNL-NCS-44945-01/04-Rev., Informal Report, Brookhaven National Laboratory, written by the members of the Cross sections Evaluation Working Group (CSEWG); edited by V. McLane, Revised April 2002.

[13] Mass and Density, Criticality Relationships, Generalized, UCRL-TR-204988, Lawrence Livermore National Laboratory, by D. E. Cullen., June 2004, available online at http://www.llnl.gov/cullen1/scaling.htm

Appendix: Author Addresses for Contact

Dermott E. Cullen
University of California
Lawrence Livermore National Laboratory
P.O.Box 808/L-159
Livermore, CA 94550
U.S.A.
Tele: 925-423-7359
E.Mail: cullen1@llnl.gov
Website: http://www.llnl.gov.cullen1

Roger N. Blomquist, ANL
Argonne National Laboratory (208-E111)
9700 S. Cass Ave.
Argonne, IL 60439
Tele: 630-252-8423
E Mail: RNBlomquist@anl.gov

Maurice Greene, ORNL
Oak Ridge National Laboratory
P.O. Box 2008
Oak Ridge, TN 37831
U.S. A.
Tele: 865-574-8712
E.Mail: greenenm@ornl.gov

Edward Lent, LLNL
University of California
Lawrence Livermore National Laboratory
P.O.Box 808/L-198
Livermore, CA 94550
U.S.A.
E.Mail: lent1@llnl.gov

Robert MacFarlane, LANL
MS B243
Los Alamos National Laboratory
Los Alamos, NM 87545
U.S.A
Tele: 505-667-7742
E.Mail: ryxm@lanl.gov

Scott McKinley, LLNL
Defense and Nuclear Technologies
Lawrence Livermore National Laboratory
L-95 LLNL
7000 East Ave.
Livermore, CA 94551
U.S.A.
Tele: 925-424-2738
E.Mail: mckinley9@llnl.gov
Website: http://www.llnl.gov/Mercury

Ernest F. Plechaty, LLNL
14738 S.W. Juliet Terrace
Tigard, OR 97224-1291
U.S.A.
Tele: 503-579-7929
E.Mail: Plechaty1@verizon.net

Jean Christophe Sublet, CEA
CE de Cadarache
Commissariat à l'Énergie Atomique
13108 Saint Paul Lez Durance
Cedex FRANCE
Tele: +33 (0)442257250
E.Mail; jean-christophe.sublet@cea.fr

University of California
Lawrence Livermore National Laboratory
Technical Information Department
Livermore, CA 94551